N69-36282

STUDY OF THE APPLICATION OF LASER TECHNOLOGY TO ATMOSPHERIC CONTAMINATION MEASURATION

JOHN U. HIDALGO
PRINCIPAL INVESTIGATOR

Radiation Laboratory
Tulane University

FINAL TECHNICAL REPORT

May 1, 1968 to April 30, 1969

Contract No. NAS 12-664

1. Air -- Contamination
2. Aerosols -- Measurement
3. Lasers

FINAL TECHNICAL REPORT

May 1, 1968 to April 30, 1969

NASA-ERC CONTRACT NAS12-664

Prepared By

Radiation Laboratory
Tulane University

For

NATIONAL AERONAUTICS AND SPACE ADMINISTRATION
ELECTRONICS RESEARCH CENTER
CAMBRIDGE, MASSACHUSETTS

John U. Hidalgo
Principal Investigator

TABLE OF CONTENTS

LIST of FIGURES and ILLUSTRATIONS

CHAPTER I

INTRODUCTION

This is a report of the activities of the Tulane University Radiation Laboratory on the project, "Study of the Application of LASER Technology to Atmospheric Contamination Mensuration" for the period May 1, 1968 to April 30, 1969. The effort has been supported under contract number NAS 12-664 from the Electronics Research Center, National Aeronautics and Space Administration.

Purpose:

The purpose of this study is to investigate the application of LASER technology to the measurement of impurities and pollutants in the atmosphere. The emphasis will be on techniques which are applicable to atmospheric probing from remote stations. The effort will be related directly to the methods and equipment under development in the Optics Laboratory of the Electronics Research Center of the National Aeronautics and Space Administration.

Study Plan:

With the cooperation of the Optics Laboratory, special LASERS will be acquired and installed. Installation will include the mounting of a LASER atop one of the taller buildings on campus and the installation of an adequate corner reflector on another tall building at a distance of over one mile. The attenuation of this folded beam will be studied and related to parallel measurements of the atmospheric pollutants and current evaluation of the meteorological parameters.

Serial measurements from this system should provide correlation of the intensity of pollution with the presumed kinetic conditions caused by local rainfall and wind variations.

This initial activity should provide the basis for a sound and convenient system for regional air management evaluation which could follow in succeeding years. The success of this measurement technique will indicate the desirability of a series of "folded path" measurements extending radially from a central location. This central location would be linked to data processing equipment for rapid evaluation and presentation. With this data available it should be possible to predict conditions and trends and relate these to expected weather conditions. If measurement granularity is sufficient it may be possible to trace the source of pollutants in the area.

Specific Program:

The sequence of activity will be in phases as follows:

1. Acquisition and fabrication of CO_2 LASERS and mount construction.

2. Establish a folded path system over a short distance (about 200 yards) in the lower atmosphere and begin calibration checks with chemical techniques.

3. Establish long folded path (about two miles) and begin serial measurements to evaluate relationships with weather patterns.

4. If time permits measurements will be made over other pathways over the city and begin the development of appropriate data acquisition and processing for application to the mathematical modeling.

CHAPTER II

SYSTEM CONCEPTS and THEORETICAL MODELS

General System Description:

The basic technique to be used here for the measurement of specif air pollutants employs the wide range of tuneability of CO_2 infrared lase Essentially a two-beam differential infrared spectrometer is established which can operate over long pathways. These CO_2 lasers can oscillate on any one of approximately 30 different infrared emission lines in the region between 9.2 and 10.7 microns, that is, the middle infrared. Many the hydrocarbons and other types of reaction products commonly classed as air pollutants show strong molecular infrared absorption in this region. In principle, a CO_2 laser can be tuned to a wavelength corresponding to an absorption line of the pollutant molecule. Thus if one measures the relative attenuation of the transmitted laser beam in the atmosphere, one can with some degree of certainty ascertain the amount of pollutant prese on the atmospheric pathway. This method presumes however, that there is no other absorbing molecule present in the atmosphere which can absorb at that particular wavelength.

Under ideal conditions only one such tuneable laser is required. By comparing the transmitted laser beam with the normalized received signal level, than pollutant concentrations down to fractions of parts of pe million can be determined. In practice however, several effects mitigate the accuracy with which this determination can be made. These effects co sist primarily of 1) laser output variations, 2) atmospheric turbulen and scintillation effects and, 3) the existence of other pollutant molecules in the atmosphere.

Also if only one laser is used, it is extremely difficult to distinguish molecular absorption from particle scattering. It is therefore preferable to use two separate lasers, one of which can be tuned to the molecular absorption line and the second tuned to an adjacent but non-absorbing region of the spectrum. Generally these two transmitted laser lines will be sufficiently close in wavelength that atmospheric turbulence, scintillation and small particle scattering will affect both beams to the same extent. Thus by a relative comparison of the absorption of the two beams, the exact amount of molecular absorption due to pollution may be determined.

The basic concept therefore, for an air pollution monitoring system consists of two tuneable carbon dioxide lasers at the transmitting site. Situated about the transmitting site are several retroreflector of fixed-mirror stations. Beams from the transmitting site sent to each of the reflecting stations are returned to the transmitting site in a fashion similar to a radar system. A dual channel receiver is employed to measure differentially the amount of absorption in each laser beam. The major problems concerning the development of a working system are, first, the development and construction of tuneable CO_2 lasers which may be adjusted to a known wavelength with accuracy; secondly, the establishment of suitable retroreflector stations about the transmitter site, and finally, the establishment of a two-channel receiver system with suitable signal processing for accurate relative measurement of the returned signals.

Measurements of Specific Pollutants:

Two of the more likely pollutants to be measured by this technique are ethylene and ozone.

Hanst[1] has found ozone absorptivity at 9.48 microns to be 3.74×10^{-4} $ppm^{-1}m^{-1}$ at 1 ATM total pressure. This absorption peak is very close to the (calculated) P(12) transition of the $00^0 1 - 02^0 0$ lasing band at 9.4882 microns. For a reference frequency an R branch transition such as R(30) at roughly 9.26 microns can be used.

The absorptivity of ethylene can be derived from published spectral data such as those of Pierson, et al.[2] Peak absorption occurs at roughly 10.6 microns and is approximately 1.13×10^{-4} $ppm^{-1}m^{-1}$. Absorption measurements could be made using the P(22) transition at 10.6118 microns. A suitable reference laser line would be the R(8) transition of the $00^0 1 - 10^0 0$ band at 10.33 microns.

The absorption of monochromatic laser radiation by pollutant molecules follows the usual exponential law,

$$LOG_{10}\, I/I_o = -\alpha\mu x \qquad (1)$$

where

- I is the power received after passage through distance x,
- I_o is the transmitter power,
- α is the monochromatic "absorptivity" in units of $ppm^{-1}m^{-1}$,
- μ is the average pollutant concentration along the path in parts per million (ppm)
- x is the path length in meters.

A typical calculation for ozone measured over a 2-kilometer total path yields the detectable ozone concentration as a function of detectable path loss, shown in Table 2-1

I/I_o	PPM
.8	.133
.9	.061
.95	.029
.98	.012
.99	.0066

TABLE 2-1 Detectable Ozone Co

Thus a system capable of measuring a 5% change in relative signal level can determine an ozone concentration of .03 parts per million. Disregarding for the moment the effects of atmospheric scintillation and the possibility of other pollutant gases in the pathway, the ultimate accuracy of the measurement depends upon one's knowledge of the molecular absorption coefficients at the laser wavelengths. Most absorption data published to date have been obtained with infrared spectrometers. The resolution of such instruments is generally quite inferior compared to the natural linewidth of the laser oscillation and thus the degree to which the laser line exactly matches a fine structure molecular resonance may not be known with great accuracy. A small wavelength discrepancy between the two lines can considerably alter the absorption coefficient. Thus it would seem most desirable to measure the absorption coefficients of the particular pollutant molecules using the tuneable laser source itself.

Long,[3] for example, engaged in a lengthy series of experiments studying absorption at laser wavelengths in the visible and near infrared. However, the tuneable CO_2 laser was not available at the time of this study and his results are of little pertinence. It is anticipated that absorption data on a variety of gases will become available as more researchers become familiar with laser technology. As a first step in this direction a 10-foot two pass gas cell was constructed into which various concentrations of pollutant gases could be introduced. This cell was completed only shortly before the termination of the contract and hence no measurements were taken.

SIGNAL and NOISE CONSIDERATIONS

For a laser beam having a power P_T, an initial beam radius of r_o and an angle of divergence of θ_o which is very small, the beam area at a distance R from the transmitter will be

$$A(R) \cong \pi(r_o + \theta_o R)^2 \tag{2}$$

If the beam intensity is ideally assumed to be uniform throughout its cross section, then the portion of transmitted power intercepted by a circular corner reflector having radius $r_c < r_o + \theta_o R$ will be

$$F_1 = \frac{\pi r_c^2}{\pi(r_o + \theta_o R)^2} \tag{3}$$

Ideally the corner reflector will return the power $F_1 P_T$ to the vicinity of the transmitter in the form of a collimated beam having diameter $2r_c$. However, imperfections in the reflector and turbulence in the intervening atmosphere will result in a beam diverging at an angle θ_c. Then a receiver having an aperture radius of r_r will receive a portion

$$F_2 = \frac{r_r^2}{(r_c + \theta_c R)^2} \tag{4}$$

of the power intercepted by the corner reflector if $r_r < r_c + \theta_c R$ and if a uniform power density throughout the beam is still assumed to exist. The average received power then will be

$$P_r = F_1 F_2 P_T \tag{5}$$

It should be noted that F_1 and F_2 both have maximum values of 1, which occur when the reflector or receiver aperture respectively is larger than the cross section of the incident beam.

Values of F_1F_2 were computed for a system having transmitter and receiver aperture diameters of 4 inches and 8 inches respectively, a corner reflector of 2.5-inch diameter and initial divergence angles of either 1 or 2 milliradians. The equivalent divergence of the reflected beam was arbitrarily set at 1 milliradian. Optical efficiencies were assumed to be 100% and atmospheric absorption was neglected. The results are given in Table 2-1 for various values of range R.

R (in 1000's of feet)	θ_o = 1 mrad P_r/P_T	θ_o = 2 mrad P_r/P_T
0.1	0.153	0.0808
0.333	0.0253	0.00910
1.0	8.01×10^{-4}	2.37×10^{-4}
2.0	5.97×10^{-5}	1.58×10^{-5}
4.0	4.15×10^{-6}	1.08×10^{-6}
7.0	4.66×10^{-7}	1.19×10^{-7}
10.0	1.15×10^{-7}	2.92×10^{-8}

TABLE 2-2. Transmission Path Power Attenuation.

From Table 2-2 it is concluded that the received signal power should be no lower than about -75 dBW for a one-watt laser output power over a two-mile path (one way). This compares favorably with the -105 dBW required to produce an output signal-to-noise ratio of 0 dB from a gold-doped germanium detector when internal noise only is considered. It should be pointed out, however, that the most sensitive range of this type of detector is in the 4-7μ range, and is less sensitive by about 8 dB at 10μ. If the detector is operated in an internal-noise-limited condition, then the output signal-to-noise ratio should be no worse than 22 dB for the ideal system described above operating at 10μ over a two-mile path.

One major deviation of system performance from that of the ideal is the presence of scintillation of received signal intensity. This scintillation is a multiplicative type of disturbance and its effect is much greater than that due to the anticipated background noise, which is additive. The scintillation arises from passage of the laser beam through a turbulent atmosphere which results in a distortion of the transmitted wave front. Thus the signal energy at the receiver is no longer uniformly distributed throughout the beam area. Furthermore, the nature of the distribution of energy changes in a random manner. Thus a receiver whose optical area does not encompass the entire beam will be subjected to varying amounts of power and the detector output will fluctuate accordingly.

The nature of this scintillation is of interest in order to know how to process the received signal so as to most efficiently extract the desired information. A number of investigators have found the scintillation to be log-normal in nature, both over one-way paths[4,5] and, more recently, over folded paths.[6] The variance of scintillation is predicted by theory[7] to increase with increasing range. However, experimental evidence appears to refute this[8,9], and it appears that although scintillation does increase up to a relatively short range, beyond this range no further increase occurs.[9]

While operating a He-Ne laser over a one-way path, Rosner[10] noted that in the received signal occasional large peaks never exceeded a maximum level, and many of them reached that level. Rosner thus concluded that the peaks represented the times when the received signal was spatially coherent over the area of the receiving optics. The peaks thus represent the received signal level in the absence of turbulence, and the average received signal power will be less than this ideal value by an amount depending on

the variance of the scintillation. Rosner found the difference between the peak value and the average value of detector output to vary widely, depending on weather conditions. On clear days the difference was about 13 dB. This was, however, over a one-way path and at much higher frequencies than those of the 10μ infrared area, where monitoring systems are to perform. Both theory[7] and experiment[6] show that the variance of scintillation decreases as frequency decreases. The use of heterodyne detection, rather than intensity detection also results in considerably poorer performance as far as scintillation is concerned.[11] Experiments over folded paths have been performed at 10.6μ[6,11]. Lucy and Lang[11] report an average fading depth of 6 dB using homodyne detection and a one-way path length of 1 km. This is approximately the same result as that obtained from data reported by Fitzmaurice et al.[6] Both groups report the scintillation spectrum to contain no significant energy at frequencies higher than about 20 Hz.

In summary, it is to be expected that log-normal scintillation will be present which must be filtered out to recover information about average received signal power. This scintillation will be subaudio in frequency, and will lower the average received signal power about 4-6 dB from that predicted for a system with no turbulence.

SYSTEM MODELS

In order to estimate and predict the performance of any complicated system it is necessary first to construct a system model which represents enough of the system characteristics with sufficient accuracy to be useful, and yet which is simple enough to allow theoretical calculations to be made. Two such idealized system models are considered here.

A typical monitoring path located arbitrarily with respect to the origin of the coordinate system is shown in Figure 2-1, with a pair of laser transmitters and receiver at point A and a corner reflector at B. If the presence of a monitorable pollutant is assumed, at point $\vec{x}$ and time t it will have concentration $c(\vec{x},t)$, where $\vec{x}$ is a position vector. The total concentration lying within the path of the folded beam will be

$$C_T(t) = 2\int_A^B c(\vec{x},t)\, d\ell \qquad (6)$$

In general $c(\vec{x},t)$ will be a random function of time, and it will be impossible to evaluate (6) analytically. Furthermore $C_T(t)$ will depend upon the positions of A and B as well as upon the overall path length L. In spite of these limitations, it appears that a good amount of insight into system performance can be obtained by studying a few idealized situations.

Ideal Two-Dimensional Two-Path System:

The first of these idealized studies consisted of a situation where a circular cloud of pollutant was carried past the monitoring path by a constant-velocity nonturbulent air stream. The pollutant concentration was assumed uniform throughout the cloud, and the cloud diameter was assumed to increase linearly with time. To further simplify calculations, the situation was reduced to two dimensions. The results of this simple idealized model were that plots giving the shape of $C_T(t)$ could be obtained by means of simple graphical and slide rule techniques for any situation it was desired to simulate.

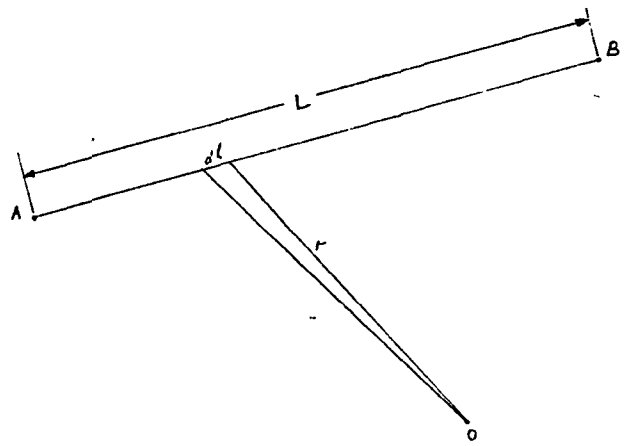

FIGURE 2-1. Monitoring Path Geometry.

This representation was used to simulate a monitoring system utilizing two beam paths of approximately the same length and about 30^{o} difference in direction. The resulting pairs of integral concentration functions were then studied to determine what useful information might be obtained from a monitoring system of this nature. The plots for a variety of situations are shown in Figure 2-2. It appears a great deal of information might be gained from the relative shapes of the two plots. The highly idealistic nature of the model structure tempers this optimism, however. The major contributions of this phase of investigation were the conclusions that 1) the most desirable orientation of the monitoring path is normal to the track of the cloud center, and 2) under reasonably general conditions cross correlation and pattern recognition studies of the two integral concentration curves might yield a good bit more information about the dynamics of the pollutant cloud than could be obtained from the record of a single monitoring path.

Pure Diffusion Model:

The second model of a pollution monitoring system was that of a horizontal path over a frictionless earth, with the pollutant entering the atmosphere from a continuously emitting point source. Spread of the pollutant is at first assumed to be by pure diffusion so that a solution to the diffusion equation holds. This model, in addition to being an exact solution for the case of pure diffusion, is also reasonably accurate for those cases where pollutant spreading is due to localized turbulence and wind currents, but where no general movement of the air mass exists.

The concentration of pollutant at a distance r from a point source continuously emitting W_o mols/sec. starting at time t = 0 is at time t

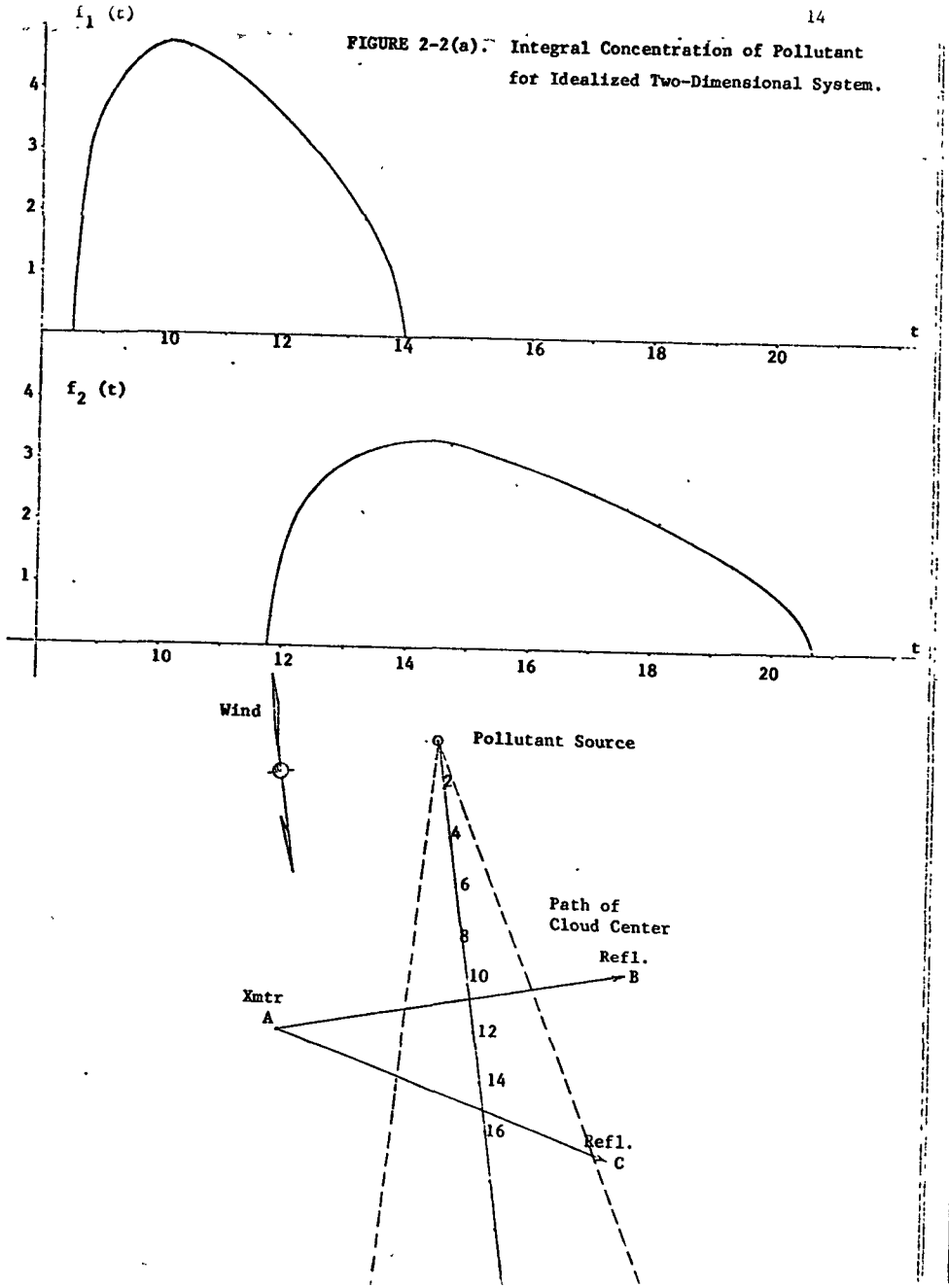

FIGURE 2-2(a). Integral Concentration of Pollutant for Idealized Two-Dimensional System.

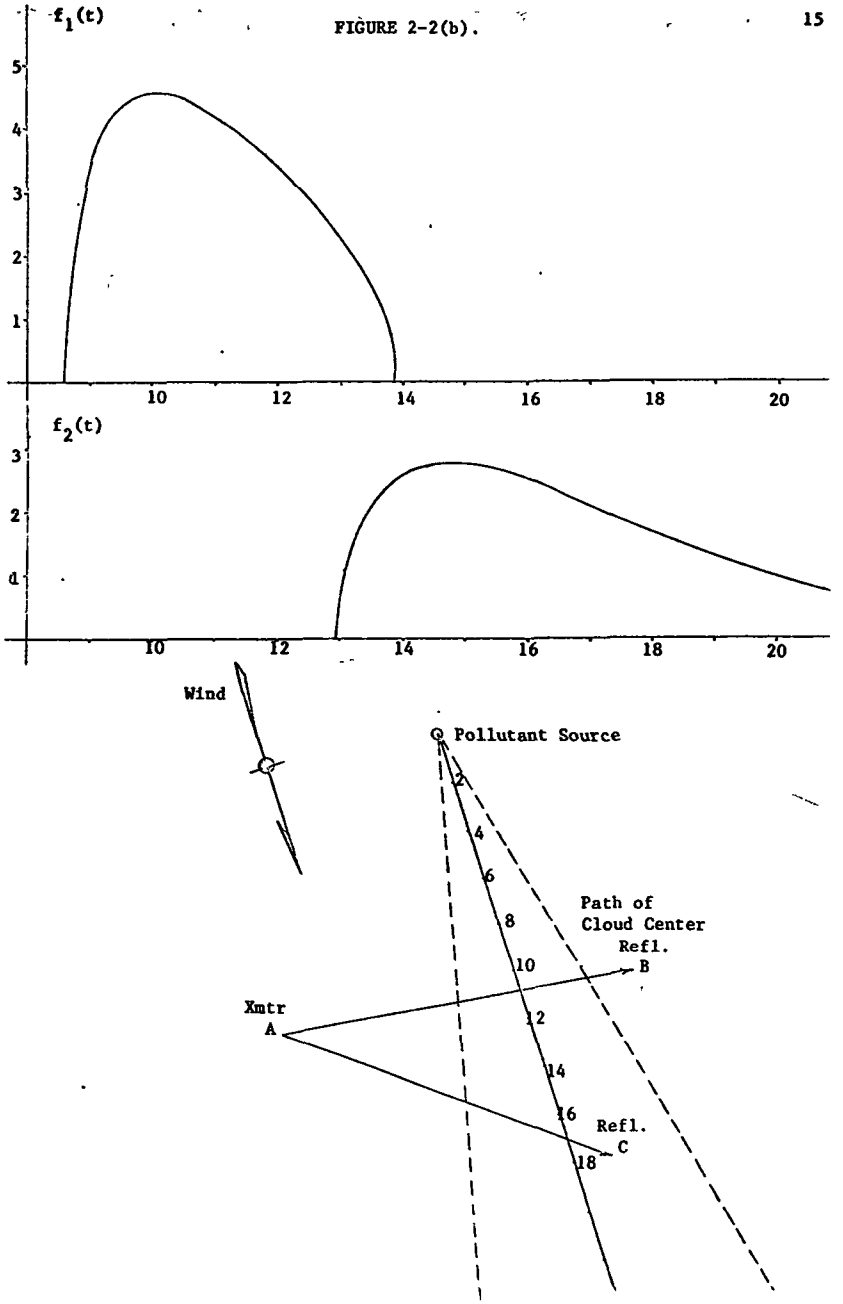

FIGURE 2-2(b).

FIGURE 2-2(c).

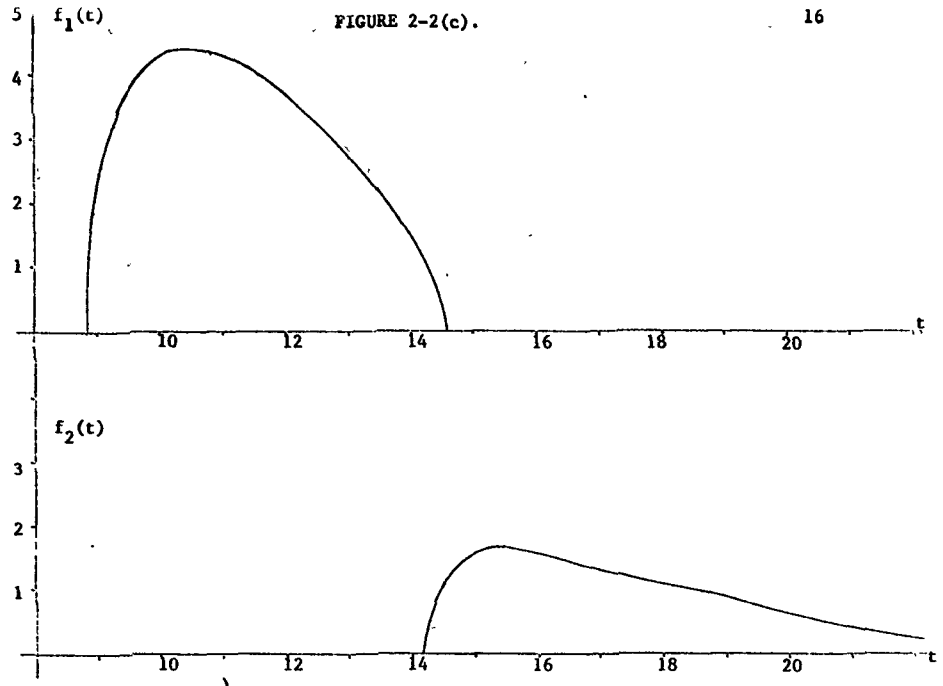

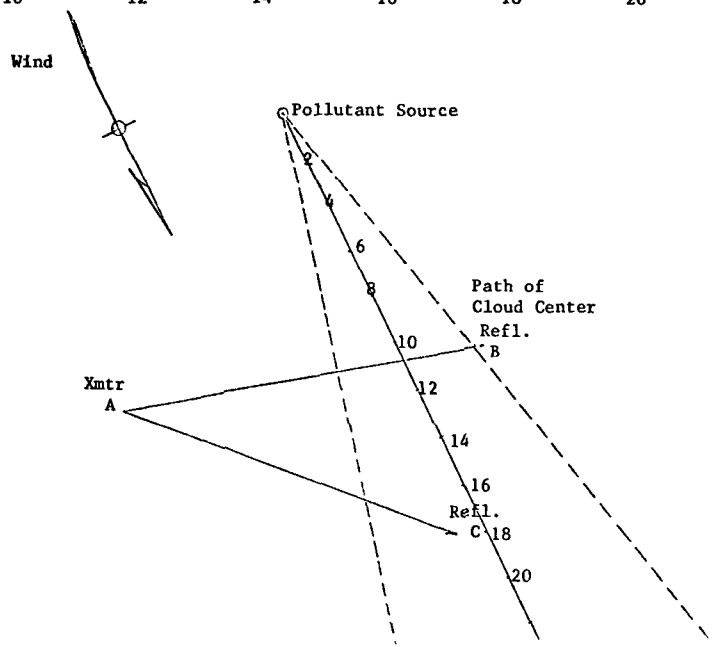

FIGURE 2-2(d)

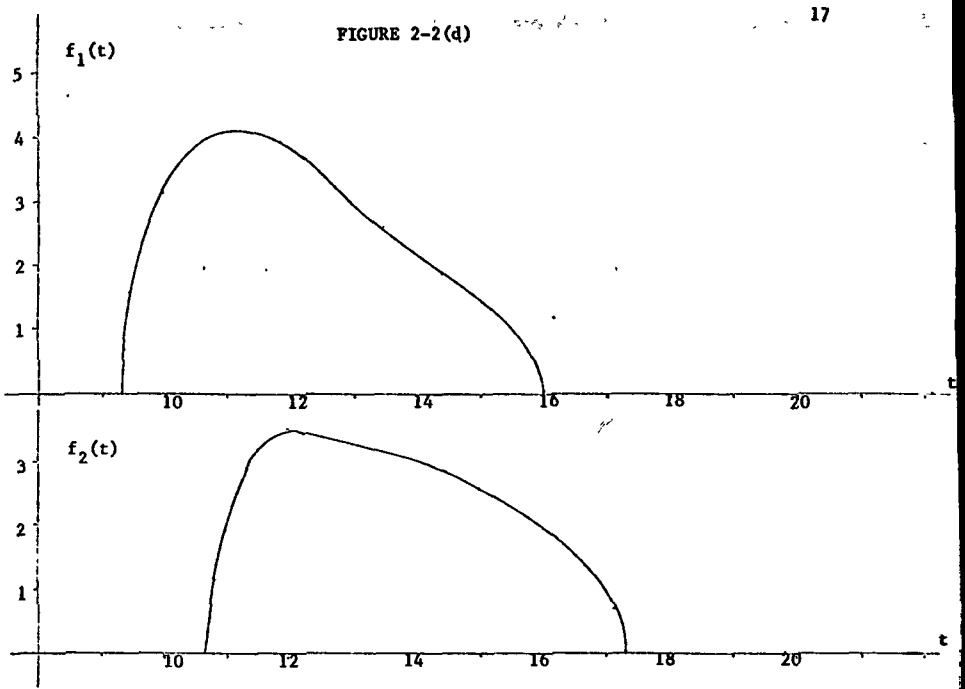

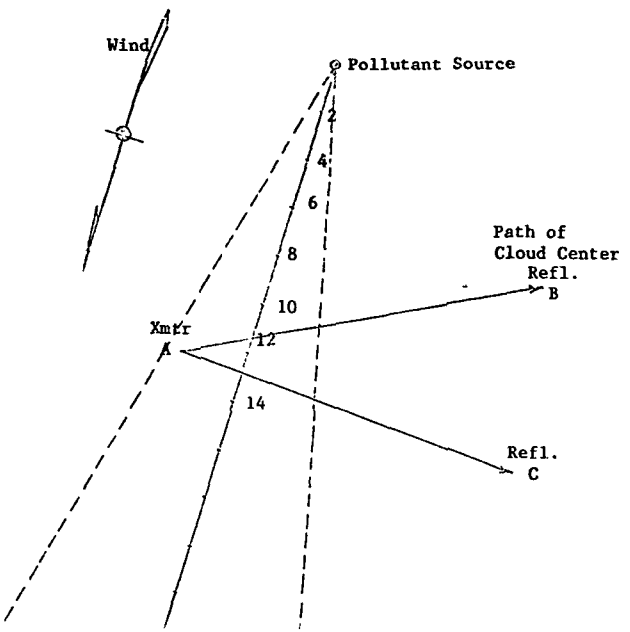

FIGURE 2-2(e)

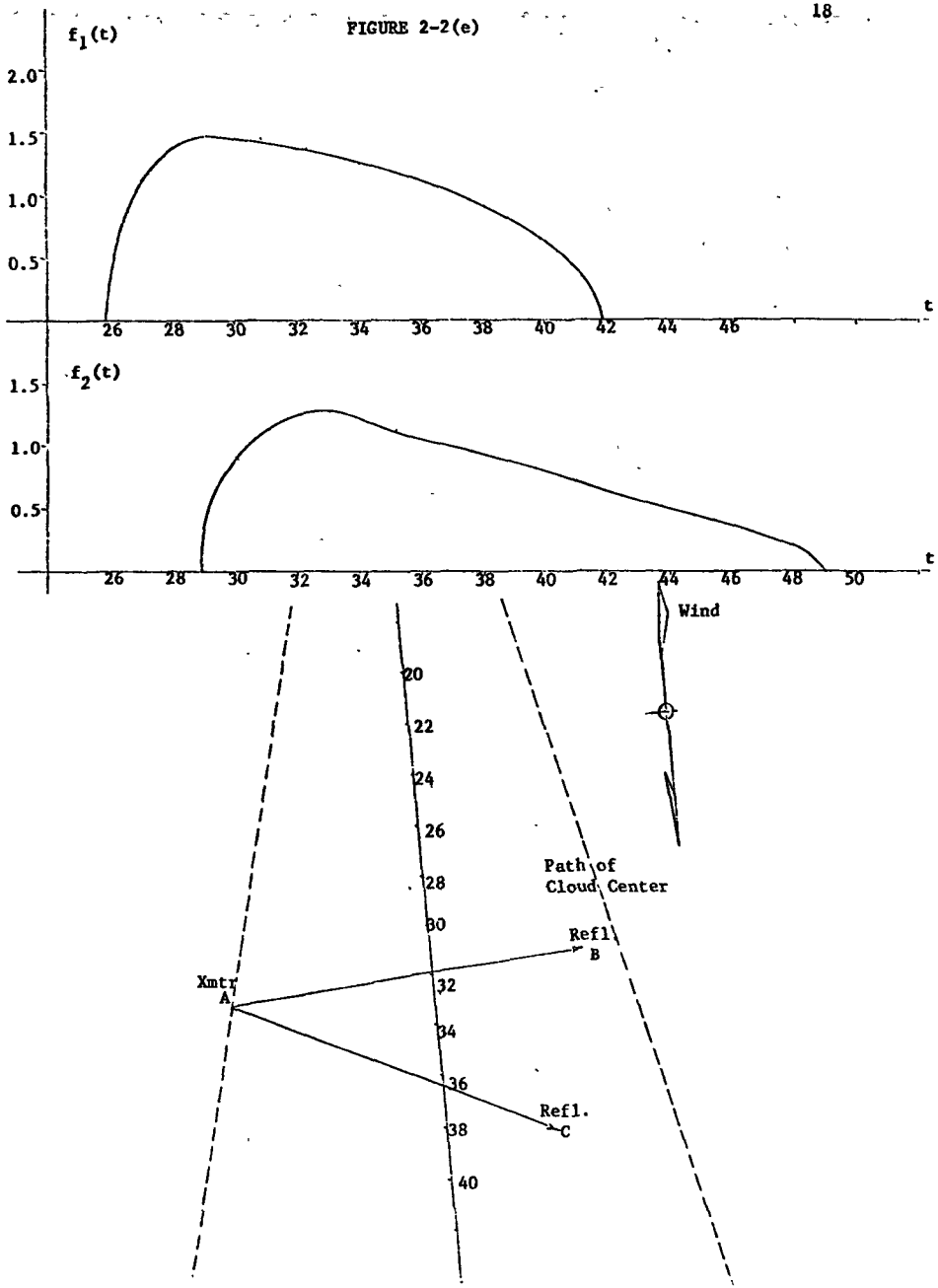

FIGURE 2-2(f).

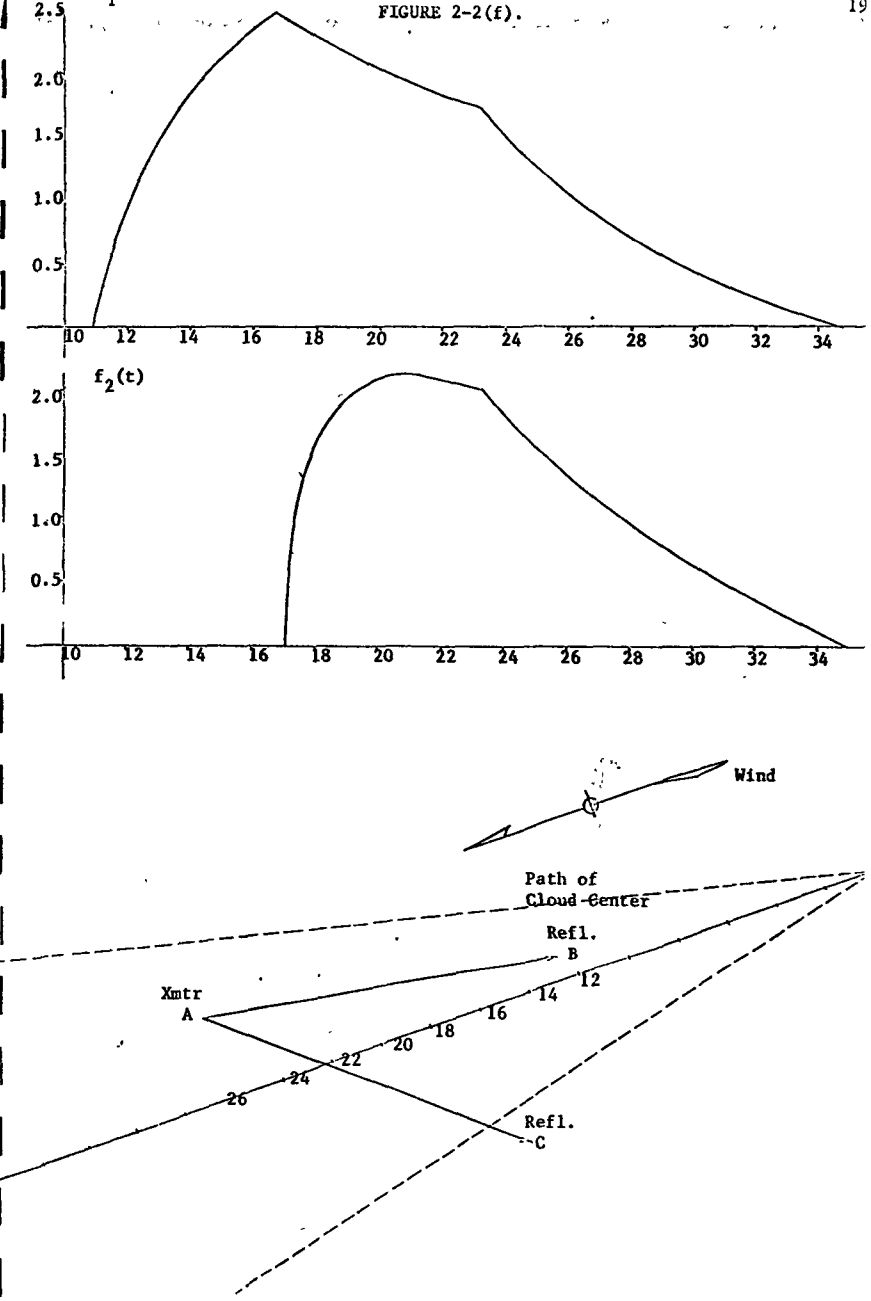

$$c(r,t) = \frac{2W_o}{4\pi D_{AB} r} \operatorname{erfc}\left(\frac{r}{4 D_{AB} t}\right) \qquad (7)$$

where D_{AB} is the diffusion coefficient for gas A (the pollutant) diffusing into gas B (the air). The factor 2 in the numerator is due to the fact that emission is into one hemisphere only (the source is assumed located on the earth's surface). All distances involved are assumed small enough that the earth's curvature need not be considered.

The substitution of (7) into (6) resulted in an integral which could not be solved analytically. Thus, all results for this system model were obtained by means of numerical solution by digital computer.

The form of $C_T(t)$ for a continuous point source having begun emission at t = 0 is typical to that shown in Figure 2-3. The vertical position of the curve and the asymptotic value for large t depend upon the location and length of the monitoring path, but the shape of the curve changes very little.

The presence of a pollutant is detected whenever the received intensity of the signal beam differs from the received intensity of the reference beam by more than F percent. The parameter F depends upon such factors as the intensity-to-noise ratio of the reference beam, accuracy in monitoring transmitted power levels, etc. The value of C_T at which detection is barely achievable is called the threshold level, C_{Th}, and is a monotomically decreasing function of F.

One measure of monitoring system performance is the time T_d at which the integral concentration C_T first passes through the level C_{Th}. This is the time lag during which the pollutant is present but remains undetected. Therefore a knowledge of T_d should be of considerable interest in system analysis.

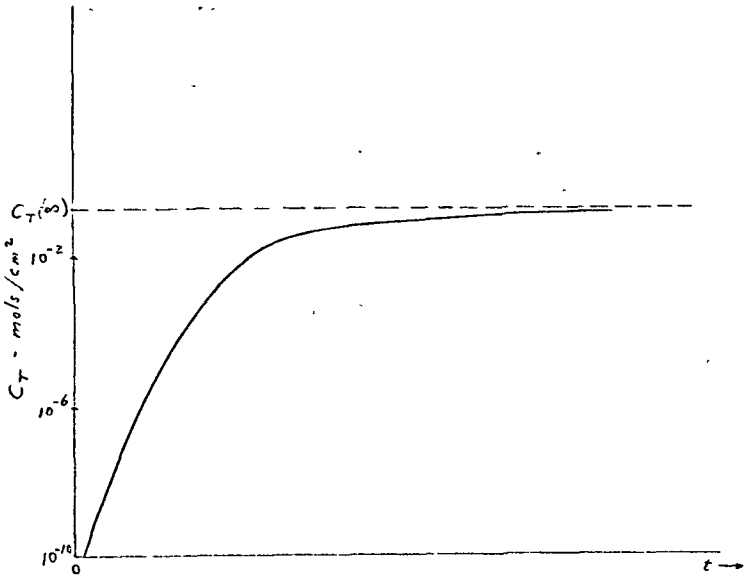

FIGURE 2-3. Typical Integral Concentration for Pure Diffusion from a Continuous Point Source.

Under the assumption that the location of the pollutant source with respect to the monitoring system may be unknown, a knowledge of T_d in all directions from the monitoring path becomes important. To effectively display this, characteristic curves were drawn joining all points with equal T_d. The resulting isochronous curves are shown in Figure 2-4 for two different values of C_{Th}. It will be noted that as the size of the curves becomes large with respect to the monitoring path length, their shape approaches that of a circle, as would be expected.

The distance from any given isochronous curve to the closest point on the monitoring path is least for positions off the end of the monitoring path. The general shape of a typical contour is approximated in Figure 2-5. The contour is straight until the end areas are reached. About the ends the contour resembles very closely an ellipse with semi-major and semi-minor axes ρ and d respectively. The closeness of this fit is indicated by the dotted lines in Figure 2-4. From the computed results, the relationship between d and ρ was found to be

$$d = \rho(1 - 0.175\, e^{-\rho/6L}) \tag{8}$$

The area enclosed by a given contour thus becomes

$$A = 2\rho L + \pi \rho^2(1 - 0.175\, e^{-\rho/6L}) \tag{9}$$

The presence of a relatively tractable formula for the area enclosed by a constant - T_d contour suggests a system optimization scheme by means of which the path length L is chosen to maximize the area A for some specified T_d.

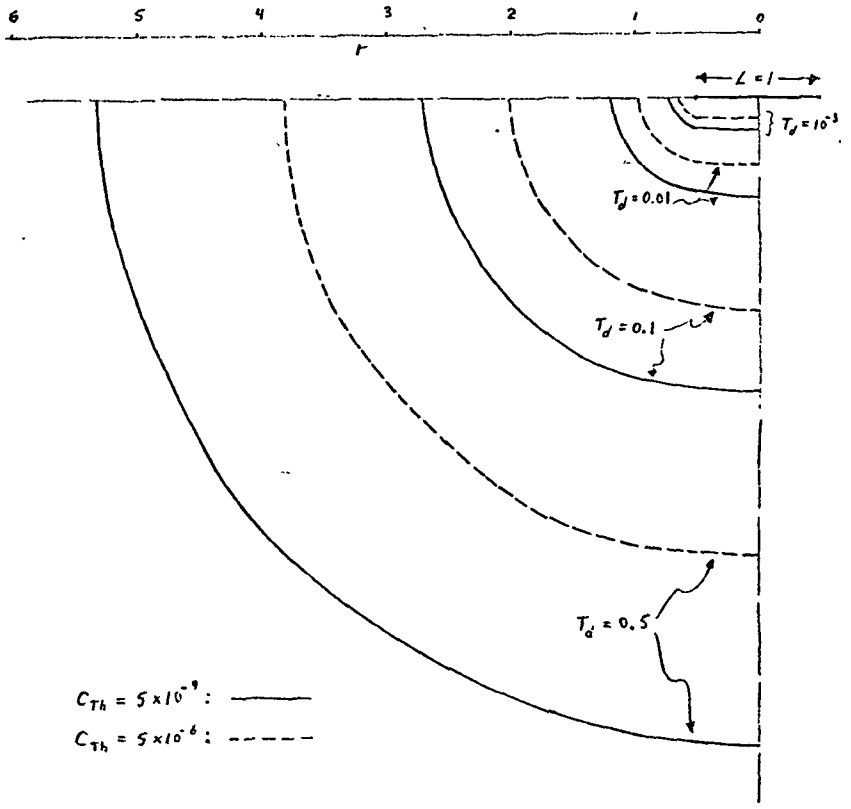

FIGURE 2-4. Isochronous Detection Contours for Unit Monitoring Path.

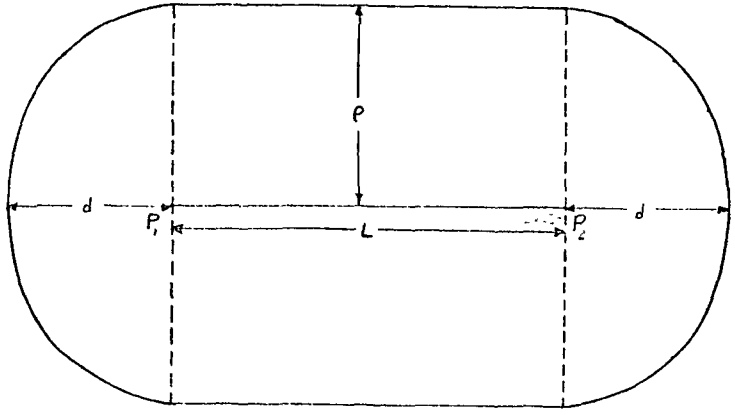

FIGURE 2-5. Approximate Geometry of Isochronous Contour.

The area A will not monotonically increase with L as might be suggested from Figure 2-5, since ρ is a function of the threshold C_{Th} as well as T_d, and C_{Th} monotonically increases with increasing L. As indicated in Figure 2-4, for constant T_d and increasing C_{Th}, ρ will decrease.

The area enclosed by curves of constant T_d is shown in Figure 2-6 for values $D_{AB} = 1$ and $W_o = 1$ in Equation (7). As a point of reference, a unit value of L was chosen as that distance for which $C_{Th} = 10^{-8}$. The necessary threshold level was assumed to increase as the fourth power of L. This is in accordance with the assumption that the received signal intensity is

$$P_r + K P_T L^{-4} \tag{10}$$

where P_T is the transmitted power and K is a system constant representing dispersion and other losses. Equation (10) holds with good accuracy for those ranges at which the reflecting and receiver optics are smaller than the diameter of the beam impinging upon them.

As seen in Figure 2-6, the area achieves a maximum for low values of T_d, thus indicating the possibility of an optimum value for L. This conclusion will be correct if area coverage is the only consideration. However, the distance ρ monotonically decreases, as shown by the dashed curves in Figure 2-6. Hence as L is increased a constant T_d contour assumes an increasingly elongated cigar-like shape. Since the contour shape, as well as the enclosed area, is changed considerably with increasing path length, it is probable that both properties, together with a consideration of the shape of the region to be monitored, must be considered in any monitoring system design.

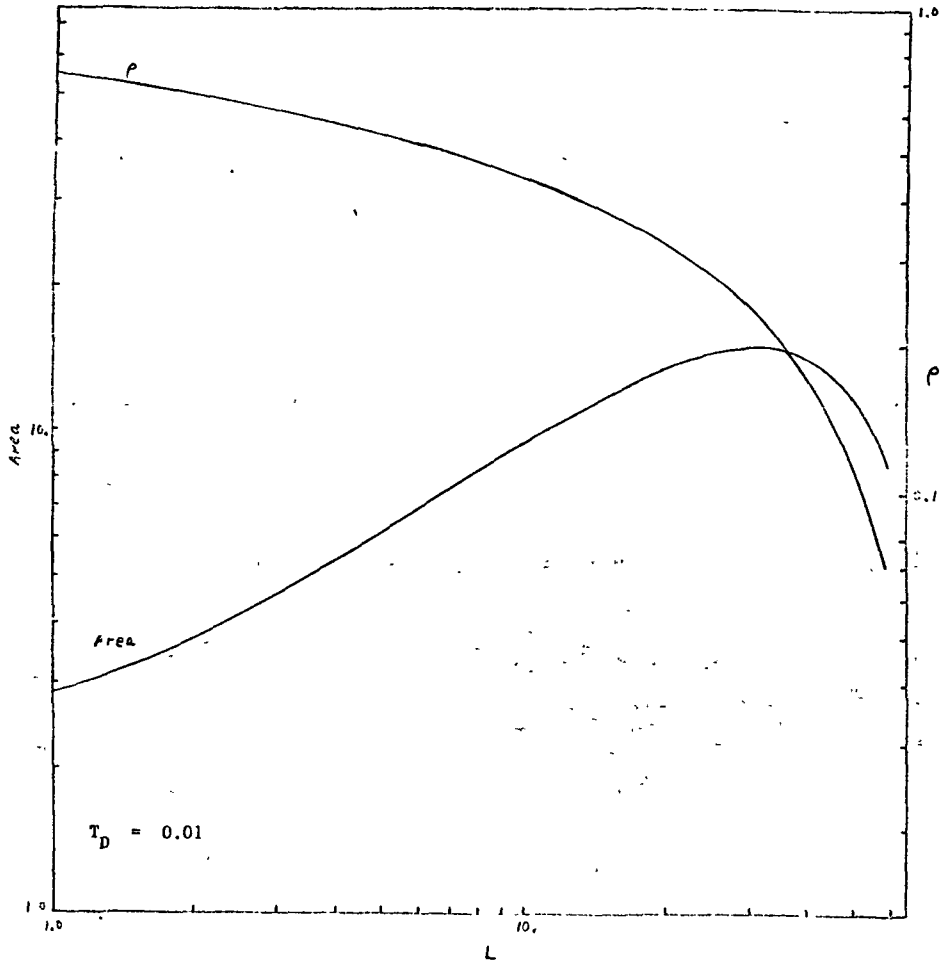

FIGURE 2-6(a). Contour Area and Radius as Functions of Path Length.

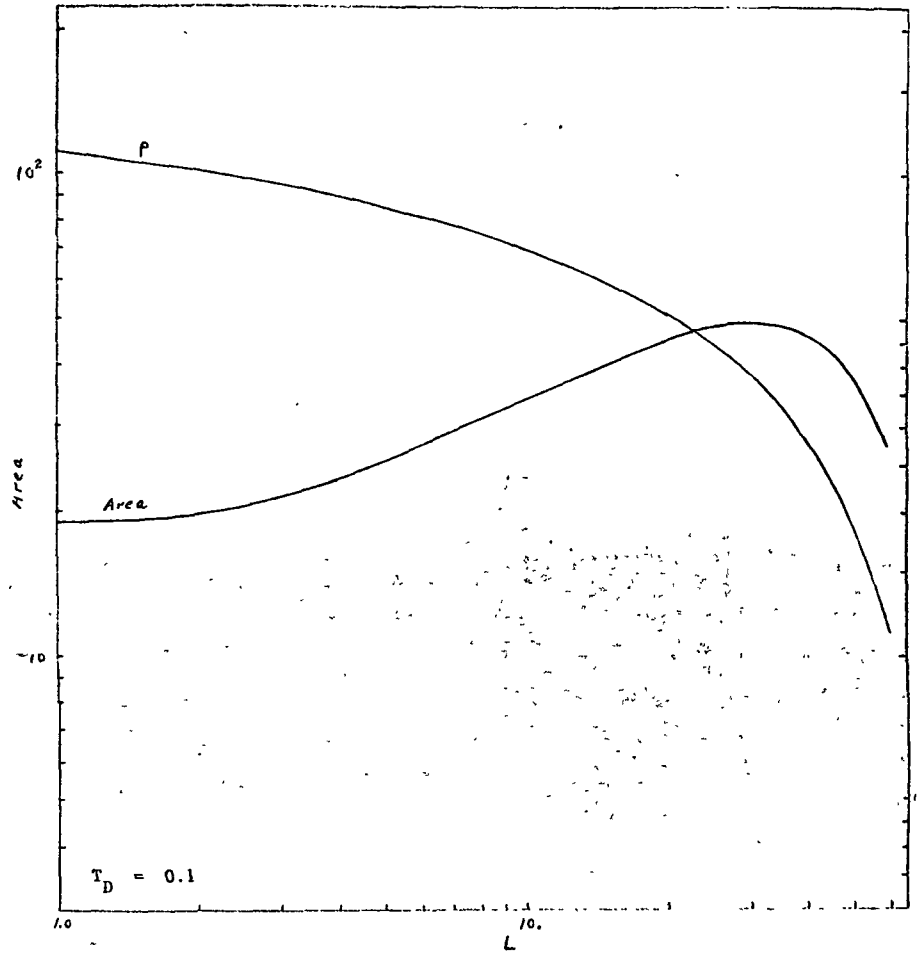

FIGURE 2-6(b).

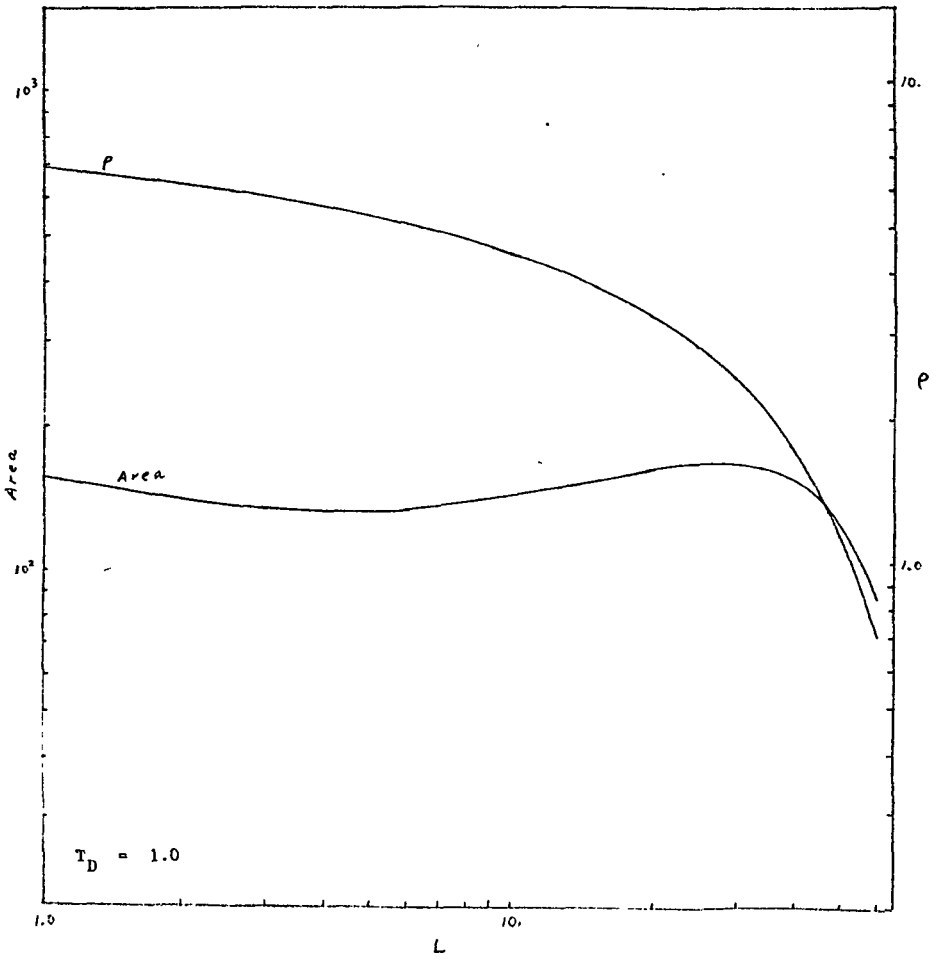

FIGURE 2-6(c).

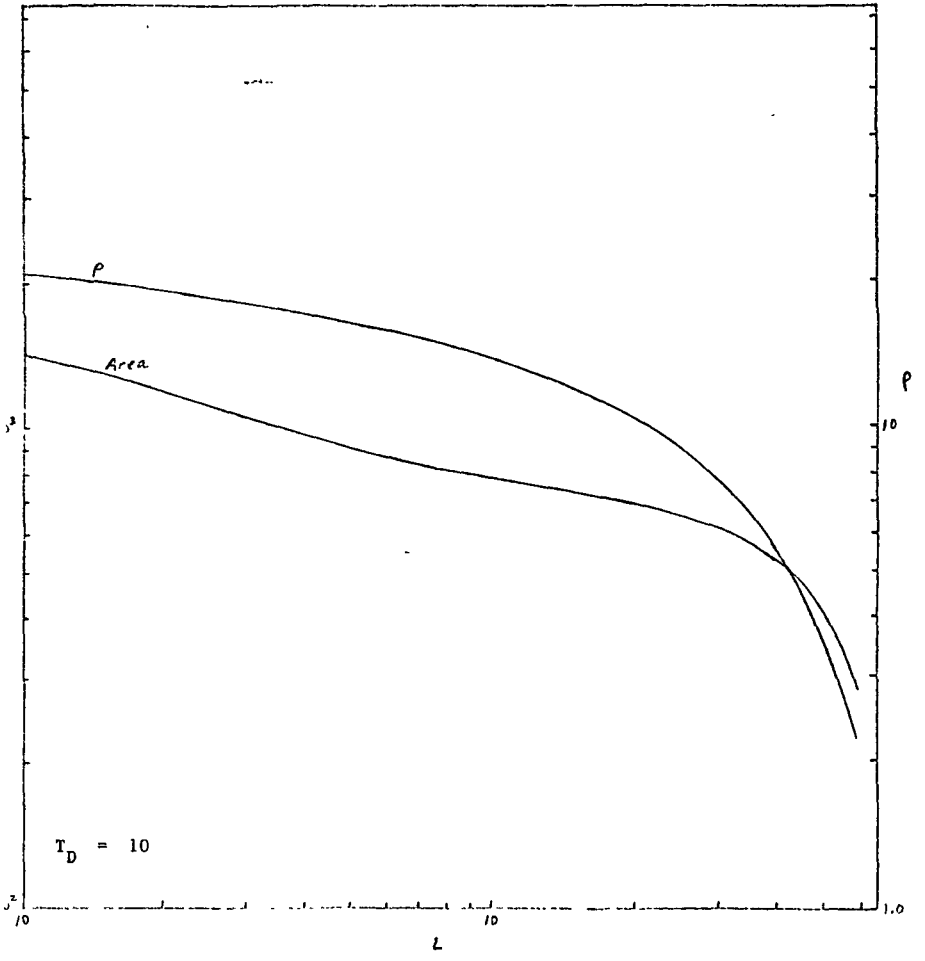

FIGURE 2-6(d).

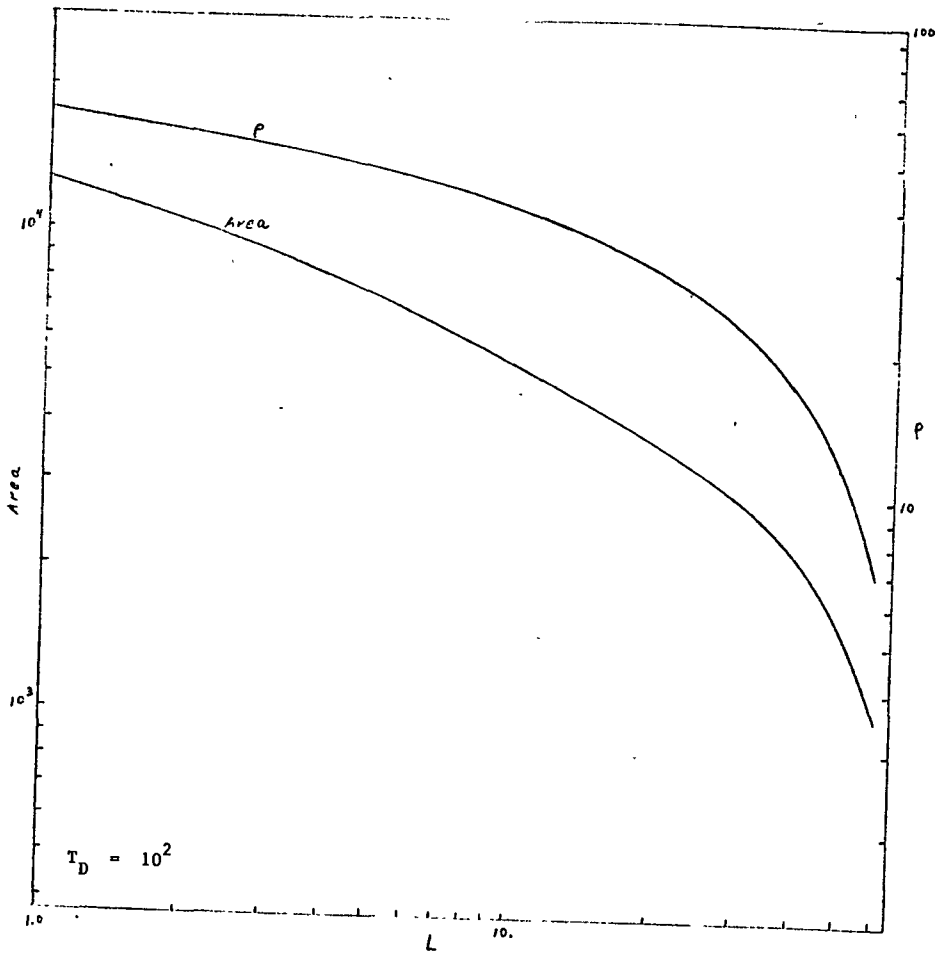

FIGURE 2-6(e).

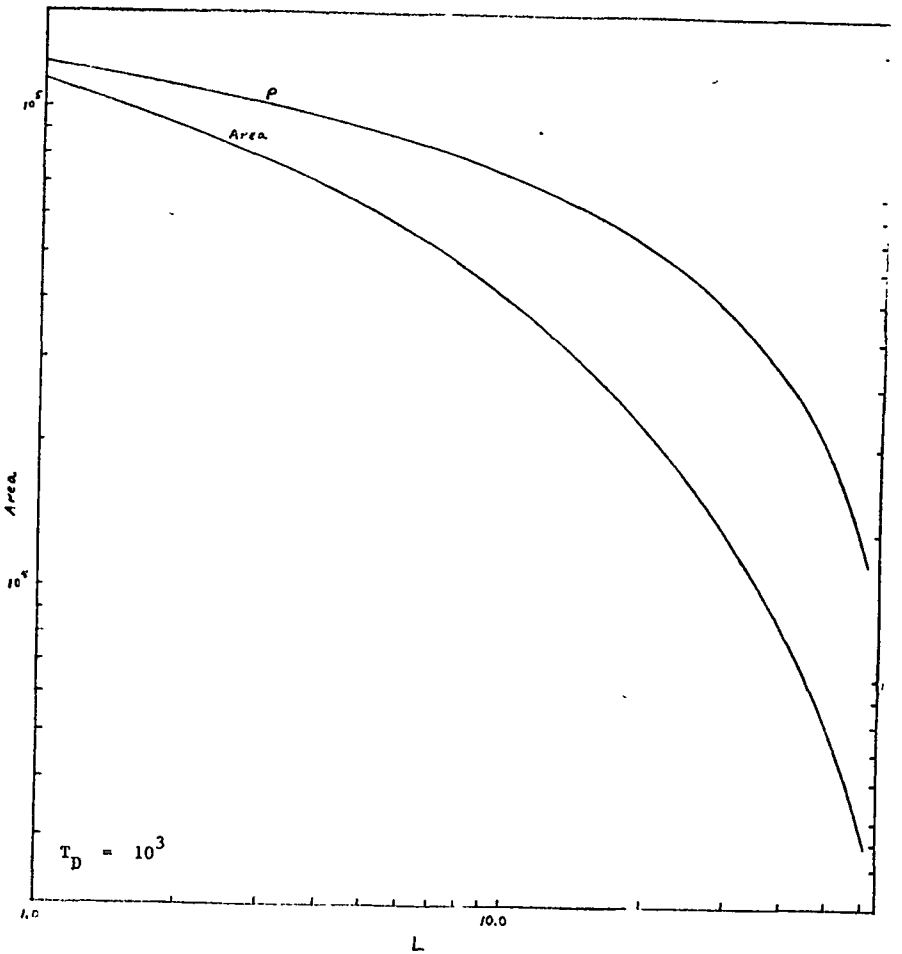

FIGURE 2-6(f).

The previous results have been obtained without reference to a particular system of units. Since monitoring systems such as are considered in this study may prove to be of considerable importance, it is desirable to know T_d in seconds when L and ρ are expressed in meters. A typical value for D_{AB} is 0.1225 cm^2/sec. for sulfur dioxide diffusing into air. Applying this value to (2) in place of $D_{AB} = 1$, as was previously used, the effect is seen to be that t will be somewhat larger for a given concentration c(r,t) to be achieved. What is perhaps more significant however, is that the dimension of r is seen to be in centimeters. Thus L = 1 implies L = 1 centimeter.

If it is assumed that a 5% absorption of the monitoring beam relative to the reference beam is sufficient to detect the presence of the gas being monitored, then from the relation

$$\exp \{-2.3026\ \alpha\mu x\} = 0.95 \qquad (11)$$

one obtains

$$\alpha\mu x = 0.0223 \qquad (12)$$

In the above, μ is the average gas concentration along the path in parts per million (ppm), x is the transmission path length in meters, and α is the gas absorption coefficient in $ppm^{-1}m^{-1}$. At the 8.8 micron absorption line for sulfur dioxide it is found that $\alpha = 4.58 \times 10^{-5}$. Thus, for 5% absorption, the required value of μx is 488. For a monitoring path length L = 1 km we have x = 2L = 2000 m, and μ = 0.244 ppm. To translate this required value of μ to a value of C_{Th}, one can use the relation that at conditions of standard temperature and pressure, a concentration of one ppm is equivalent to 4.46×10^{-11} mol/cm^3.

Thus the required average value of c(r,t) over the path is $c(r,t)_{av} = 0.244 \times 4.46 \times 10^{-11} = 1.09 \times 10^{-11}$ mol/cm^3, and the resulting value of C_{Th} is 1.09×10^{-6} mol/cm^2.

Pure gaseous diffusion is never likely to play a major role in the spreading of contaminating gasses into the air. To see that this is so, the value of c(r,t) was calculated from (2) for sulfur dioxide diffusing into air at a rate of one mol/sec. from a point 1 km away from a monitoring path one km in length. The time required for the point on the path closest to the source to reach the level of 1.09×10^{-11} mol/cm^3 determined above was $t = 2.06 \times 10^9$ sec. Somewhat smaller distances may be utilized and still considered practical from a monitoring standpoint, but the times required for pure diffusion gas spreading are never small enough to be of value.

Much larger values of D_{AB} are encountered when the diffusion process is used to account for the spreading of a gas due to local turbulence, eddys, etc, as will be discussed in the section entitled Meteorological Considerations. Then D_{AB} is called a turbulent diffusion coefficient, and a value of $D_{AB} = 10^4$ is realistic. If this value is inserted into (2) with $r = 10^5$ and $W_o = 1$, it is found that a concentration of 1.09×10^{-11} mol/cm^3 was reached at $t = 1.5 \times 10^5$ sec. This is still long, being in the order of 42 hours. Larger emission rates decrease the time required, but $W_o = 10^4$ mols/sec. is required before the desired concentration is reached in approximately 4 hours.

Application of the diffusion equation to diffusion through turbulence near the earth's surface suffers due to the fact that D_{AB} is no longer the same in all directions, being greater in a horizontal direction than it is in the vertical direction.

It may be possible in practice to approximate this effect by increasing W_o to account for the greater concentration of pollutant at or near the same elevation as the pollutant source.

Reduction of the system dimensions by one order of magnitude to L = 100 meters does not change the value of C_{Th} for a 5% minimum detectable absorption. However, a sulfur dioxide source 100 meters away on the perpendicular bisector of the path will result in C_{Th} occurring within 15 minutes for an emission rate of 4.86 mols/sec., or within 30 minutes for an emission rate of 0.85 mols/sec. These certainly appear to be acceptably small time lags in a pollution monitoring system.

The applicability of the simple diffusion equation to the study of any system depends in the end on how well it describes the existing situation. Certainly a great deal more study of meteorology and gas dynamics near the earth's surface is needed. However, the pure diffusion model represents a tractable solution which, when used judiciously with bulk transport solutions, should predict system performance to within acceptable degrees of accuracy.

METEOROLOGICAL CONSIDERATIONS

The transfer of pollutants in the atmosphere is largely dependent upon the meteorological characteristics of the lower atmosphere above the area in question. Pollutants may be transferred by molecular diffusion in a still, stable atmosphere or by turbulent or eddy diffusion in a dynamic or unstable atmosphere. Turbulent conditions usually prevail but pollution problems become severe when dispersion is by molecular transport.

Many diffusion models and equations have been developed which are usually specific to a given area under certain meteorological conditions. At present there is no quantitative way of including all variables and there is a need for more work in this area.[12]

The transport of a pollutant by molecular diffusion is dependent upon a diffusion coefficient and the gradient of concentration.

$$J_A = -C D_{AB} \nabla X_A \qquad (13)$$

where,

J_A = molar flux relative to mean motion

C = molar concentration

D_{AB} = diffusion coefficient, a parameter for each gas pair which depends on temperature and pressure

∇X_A = mole fraction gradient of component A.

Turbulent transport is much more complicated since it consists of gross movement of large numbers of molecules which are called eddys. At present there is no complete mathematical description of turbulence although considerable work has been done for a considerable length of time. Thus, empirical methods have been used to describe turbulent processes. One such method has been the use of a turbulent diffusion coefficient or eddy diffusivity defined in a manner analogous to the molecular diffusion coefficient.

$$J_A^t = -C D_{AB}^t \nabla X_A \qquad (14)$$

The eddy diffusivity is not a molecular property as is the molecular diffusivity and is a function of position and degree of turbulence.

It varies with height above the ground and the lateral diffusivity is larger than the vertical since vertical movements are damped by the earth's surface. It is also much larger than the molecular diffusivity by several orders of magnitude.

Large scale transport may be accomplished by eddys generated by slow (mechanical) or generated by thermally induced turbulence. Mechanical turbulence near the earth is dependent on the wind velocity and the type of surface. Thermal motion depends upon the vertical temperature profile and its relation to the adiabatic lapse rate. The adiabatic lapse rate is the temperature a volume of air displaced upward will assume as it encounters the lower pressure if no heat is added or removed. If the temperature of the air volume is greater than the surrounding air, the density will be less and the volume will be accelerated upward. This condition is termed instability. The converse is true if the temperature of the volume is less than that of the surroundings. Normally, the temperature of the atmosphere decreases with height ar a rate of about 1^{o} C/100 meters. At certain times as the earth's surface is cooled by loss of heat by radiation, an inversion forms and the temperature increases with height for distances which may be as great as 1500 feet.

The study of atmospheric turbulent diffusion has centered around the study of the flow characteristics of the lower atmosphere. Due to the exchange of momentum between flowing air and the earth's surface, the velocity increases with height. An accurate description of the velocity profile is necessary for diffusion studies. Several equations have been proposed, the most widely used being the power law.

$$u = u_1 \left(\frac{z}{z_1} \right)^p \tag{15}$$

which is good for layers several hundred feet in thickness (Stern). A reference velocity (u_1) at some reference height (Z_1) must be known as well as the exponent (p) which varies between zero and unity and increases with stability.

Early diffusion studies utilized a constant eddy diffusivity and consequently resulted only in order of magnitude descriptions since the diffusivity increases with height. The most commonly used expression for this variation in height is

$$D^t = D_1{}^t \left(\frac{z}{z_1} \right)^{1-p} \tag{16}$$

which is in agreement with the power law velocity profile. Sutton[14] utilized this equation and proposed an equation which is quite widely used.

$$C = \frac{Q}{\pi C_y C_z u x^{2-n}} \; e^{\frac{-y^2}{C_y{}^2 x^{2-n}}} \left[e^{\frac{-(z-h_e)^2}{C_z{}^2 x^{2-n}}} + e^{-\frac{(z+h_e)^2}{C_z{}^2 x^{2-n}}} \right] \tag{17}$$

C = gas concentration, mass/unit volume

Q = mass emission rate, mass/unit time

C_y, C_z = parameters related to the turbulent diffusion coefficients, $(\text{length})^{n/2}$

h_e = height of cloud axis at a given downwind distance

u = mean wind velocity at the given position

x = downwind distance

y = lateral distance

z = vertical distance

n = exponent in power law expression for velocity

$$u = u_1 \left(\frac{z}{z_1} \right)^{\frac{n}{2-n}} \qquad (18)$$

This equation is for a continuous point source which has been emitting for some time.

Another form of the above equation uses a standard deviation of the horizontal and vertical concentration distributions which is considerably more flexible because it doesn't depend on a power law velocity profile. The parameters appearing in Sutton's equation are empirical and must be determined by a study of the individual area over a long period of time which includes a complete range of conditions. This type of study cannot be obtained in less than a year and requires trained personnel to design and conduct the experiments.[12]

Recent work[13] has focussed attention on the Richardson Number in characterizing turbulence.

$$R_i = \frac{g}{\theta} \quad \frac{\partial\theta/\partial_z}{(\partial u/\partial_z)^2} \qquad (19)$$

where,

R_i = Richardson number

g = acceleration of gravity

u = velocity

θ = potential temperature

The potential temperature is the temperature a volume of gas would attain if brought adiabatically to a standard pressure.

The potential temperature may be related to the actual temperature by

$$\theta = T + \gamma z \qquad (20)$$

where,

T = actual temperature

γ = adiabatic lapse rate

In a stable atmosphere the Richardson Number does not vary with height. By using a temperature function, a measure of thermal turbulence is included.

In the study covered by this report no attempt was made to determine experimentally the meteorological conditions and consequently the numerical constants appearing in the many models which have appeared in the literature. As mentioned previously, attention was directed toward a study of the placement of the lasers for best utilization using the solution for molecular diffusion from a continuous point source. The diffusivity was assumed constant and both molecular and turbulent values[14] were used with no mean motion. The experience gained from this study will be of considerable help in the extension of the work to more realistic models after the meteorological information is determined.

CHAPTER III

EQUIPMENT DESCRIPTION and PERFORMANCE

As mentioned in Chapter II the monitoring technique under study requires two individually tuneable-CO_2 gas lasers, a sensitive infrared receiver, electronics for signal processing, and remote beam reflector stations. A basic block diagram of the system is shown in Figure 3-1 and is discussed more fully below.

MECHANICAL DETAILS of LASER TRANSMITTER

The laser employed is patterned after the design of Hanst et al and consists essentially of a one-meter discharge tube with an integral water jacket and a surrounding gas reservoir.[15] The laser construction is of pyrex glass and the reservoir volume is approximately five liters. The partially transmitting front window is internally mounted while the rear window is a sodium chloride flat fixed at Brewster's angle. The rear totally reflecting mirror is a one-inch diameter gold-coated spherical mirror of three meters radius of curvature. The front window is an Irtran-II flat which has been 50% aluminized. The laser operates using Matheson pre-mixed gas mixture of CO_2-N_2-He in the ratio of 1:2:17 at a pressure of 15 torr. An output power of up to five watts has been obtained in the free running mode. Excitation is normally by a 12 kilovolt, 30 MA neon sign transformer, although DC at 15 kilovolts has also been used. The lasers are cooled by flowing water through a jacket surrounding the discharge tube. At present the discharge electrodes are common neon sign electrodes although there is increasing evidence that platinum or other non-reacting electrodes would be superior.

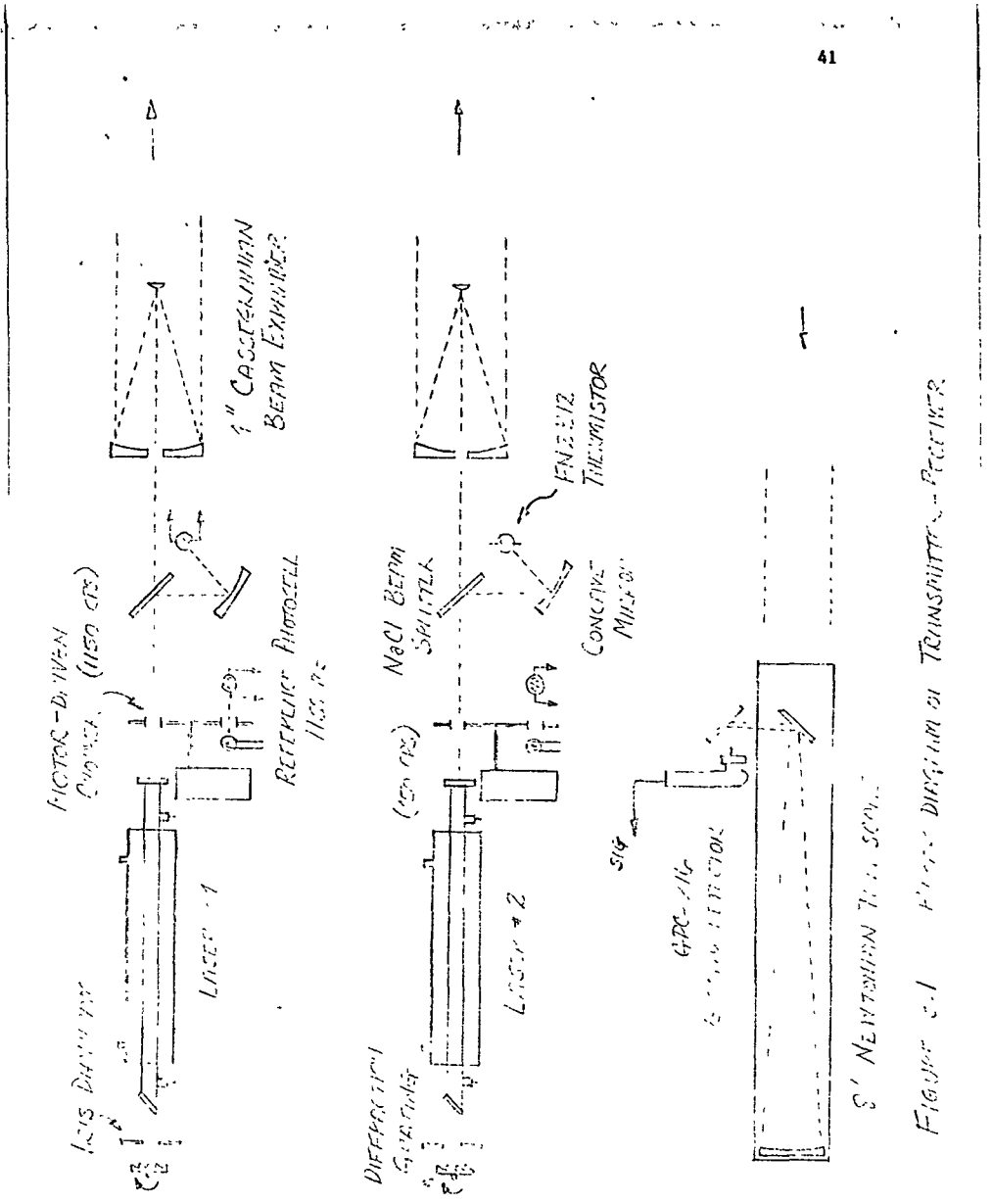

FIGURE 3-1 A BLOCK DIAGRAM OF TRANSMITTER - RECEIVER

The glass laser tubes are each rigidly mounted in a tubular box frame assembly which is approximately 6 inches square by 72 inches long. The four tubular frame members are of one-inch OD by .093 wall stainless steel No. 410 tubing. Although more desirable, Invar tubing was not obtainable in the small quantities needed here. The frame cross-members are of one-inch thick aluminum and are similar to the configuration employed by the NASA-ERC. The frame is so designed that it accomodates the laser together with the front and rear mirror adjusting mechanisms, a sodium chloride beam splitter with the output power monitoring device, the mechanical beam chopper, and finally provisions for Cassegranian beam-expanding optics. A photograph showing the complete assembly is given in Figure 3-2.

Beam Choppers:

Attached to each laser frame assembly are mechanical beam chopping devices of relatively standard configuration. Two circular aluminum disks 6 inches in diameter are mounted directly on Bodine synchronous motors. One disk has 20 equally spaced slots and is driven at 3600 rpm. The second disk has 15 holes and operates at 1800 rpm. Thus beam chopping frequencies of 1200 and 450 H_z are obtained. Chopper action is monitored by a LS-400 silicon photodetector which, together with a small lamp, serves to furnish the synchronous reference signal to the lock-in amplifier.

Output Power Monitors:

After passing through the chopping blades the laser beam is incident upon a thin sodium chloride flat mounted at 45°. This flat reflects approximately 1% of the beam into a 25 mm by 33 mm fl concave first-surface mirror.

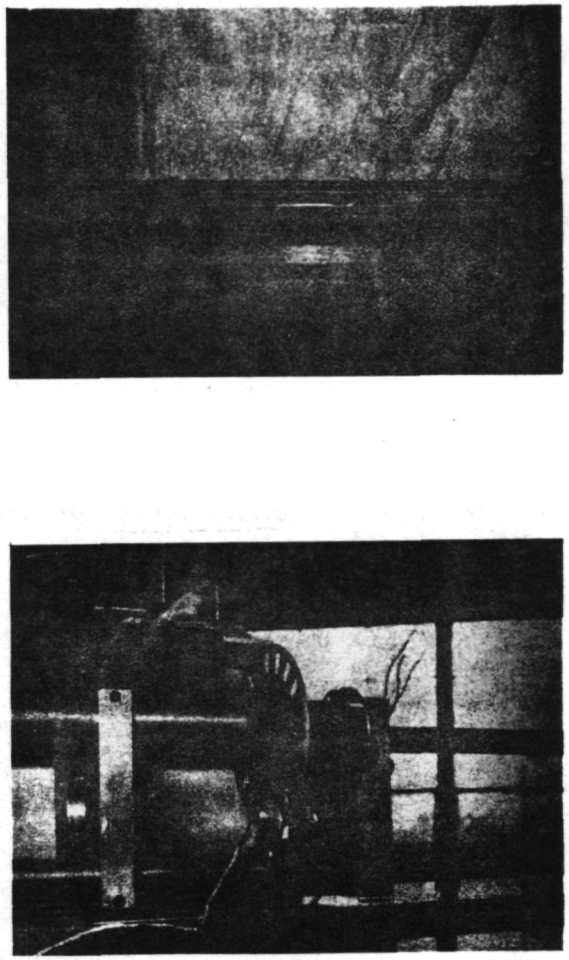

FIGURE 3-2. Laser Transmitter Assembly Including Beam Chopper.

A VECO FN2 B12 substrate-backed thin-film thermistor (Thinistor) is placed at the mirror focus. The thinistor time constant is quite short due to its high conductivity backing and low sensitive mass and it can respond to beyond 1 kilohertz. The thinistor output signal can be monitored with an ordinary AC millivoltimeter. Calibration is accomplished by plotting AC millivolts versus net laser output power as measured on a Coherent Radiation Laboratories Model 201 Power Meter. A photograph of the assembly is shown in Figure 3-3 and a typical calibration curve is given in Figure 3-4. For accurate power monitoring the laser must be operating with a stable mode configuration.

Wavelength Control:

Although original plans were to tune the laser wavelengths using the absorption gas principle described by Hanst, it has been found in practice that much more accurate control can be achieved by using an intracavity diffraction grating in place of the rear totally reflecting mirror.

We have used a 57-line/mm blazed diffraction grating obtained from the Ealing Corporation. This grating, originally aluminized, was coated with a thin layer of gold to improve reflectivity in the middle infrared region. Substantial reduction in output power was noticed when operating on a single line as compared with multiple line operation. However, the present output power of up to a watt on individual high-gain lines is sufficient for the path lengths intended. Further discussion of grating performance is found below.

Beam Expanding Optics:

The beam-expanding Cassegranian telescope is essentially a pair of concentric gold-coated spherical mirrors; one concave and one convex.

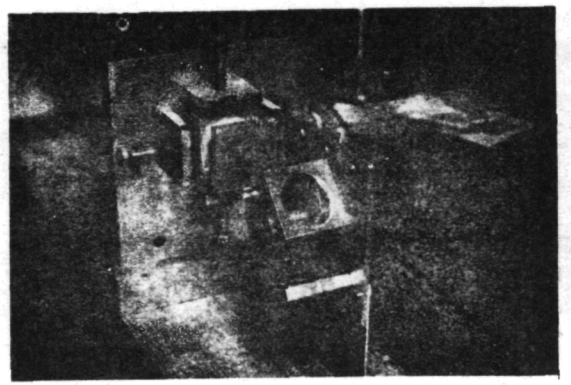

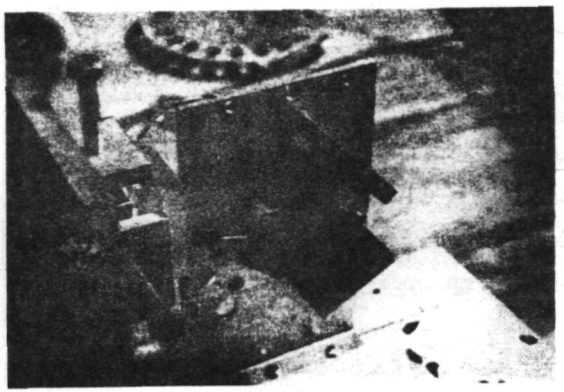

FIGURE 3-3. Laser Output Power Monitoring Device.

Page Intentionally Left Blank

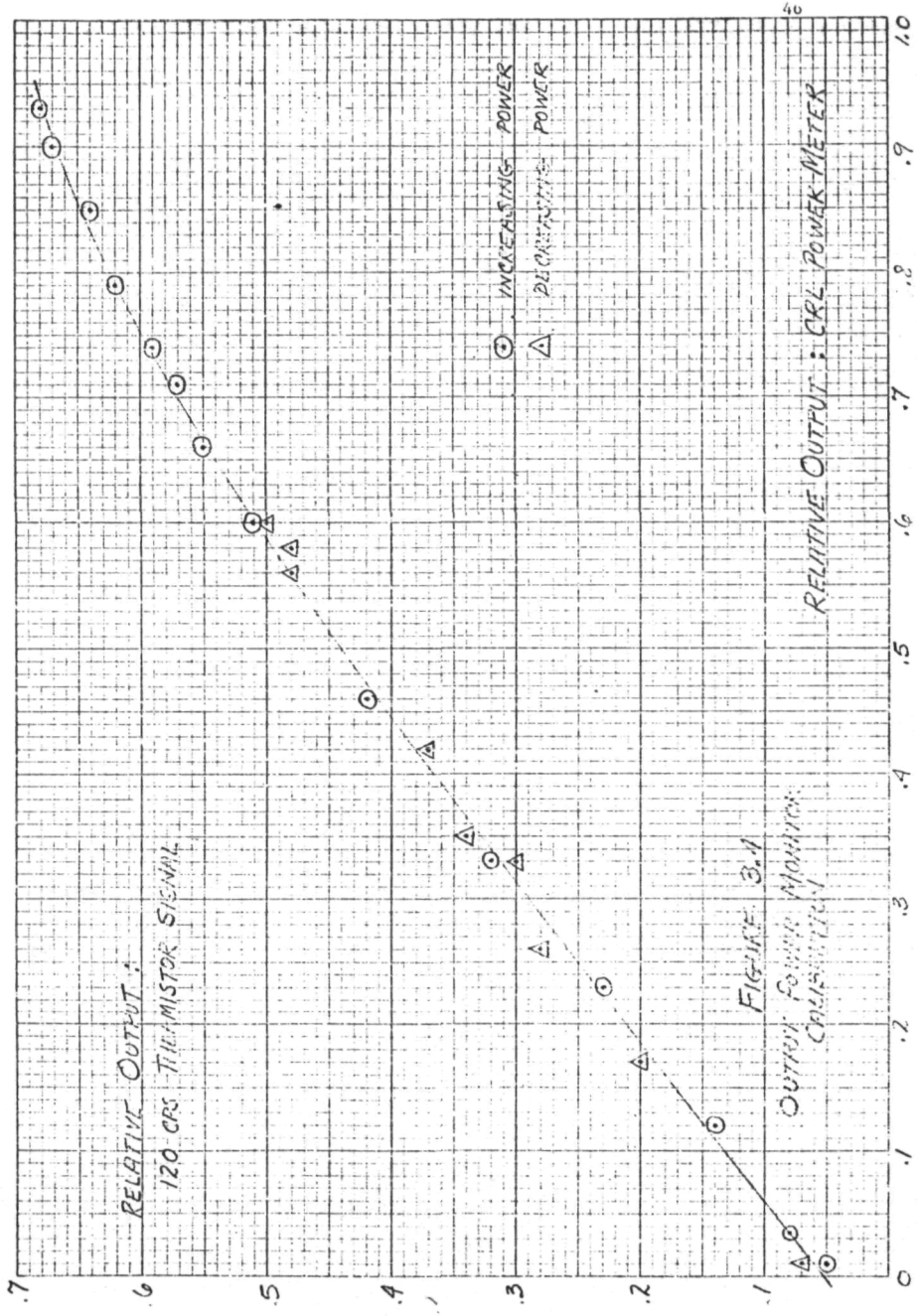

FIGURE 3-4

The primary mirror is 4 inches in diameter with a 3/8" aperture while the secondary mirror is 3/8" diameter. By allowing for a small axial adjustment of the secondary mirror the laser beam may be collimated as desired.

The laser frame assembly thus becomes a complete functioning transmitter unit with the laser, beam chopper, output monitor, to the beam expanding telescope. In addition, below each salt flat is a 240 ohm 7-watt resistor which serves as a small local heater to keep the sodium chloride from deteriorating. The performance of the unit is described in the following sections.

LASER OPERATING CHARACTERISTICS

The newly assembled lasers were filled with the pre-mixed gas mixture of 5% CO_2, 10% N_2, and 85% He to an operating pressure in the neighborhood of 10 torr. Excitation was by conventional neon-sign transformer rated at 15 kv and 30 milliamperes. Ballast resistors of 50 k ohms were inserted in the electrode arms and the excitation was balanced with respect to ground potential. Over a period of several months, numerous experiments were performed in an effort to optimize the gas pressure, excitation current and gas mixture ratios for best operation of the laser. A typical series of curves indicating the variation of output power with discharge current for various pressures of filling gas is shown in Figure 3-5. A maximum of just under five watts was recorded at a pressure of 14 torr. Up to 6.8 watts has been observed in some experiments. During early experiments the laser operation appeared stable and fairly reproduceable. However, with time the laser became much more critical in operation and output powers above three watts could only very rarely be achieved.

Page Intentionally Left Blank

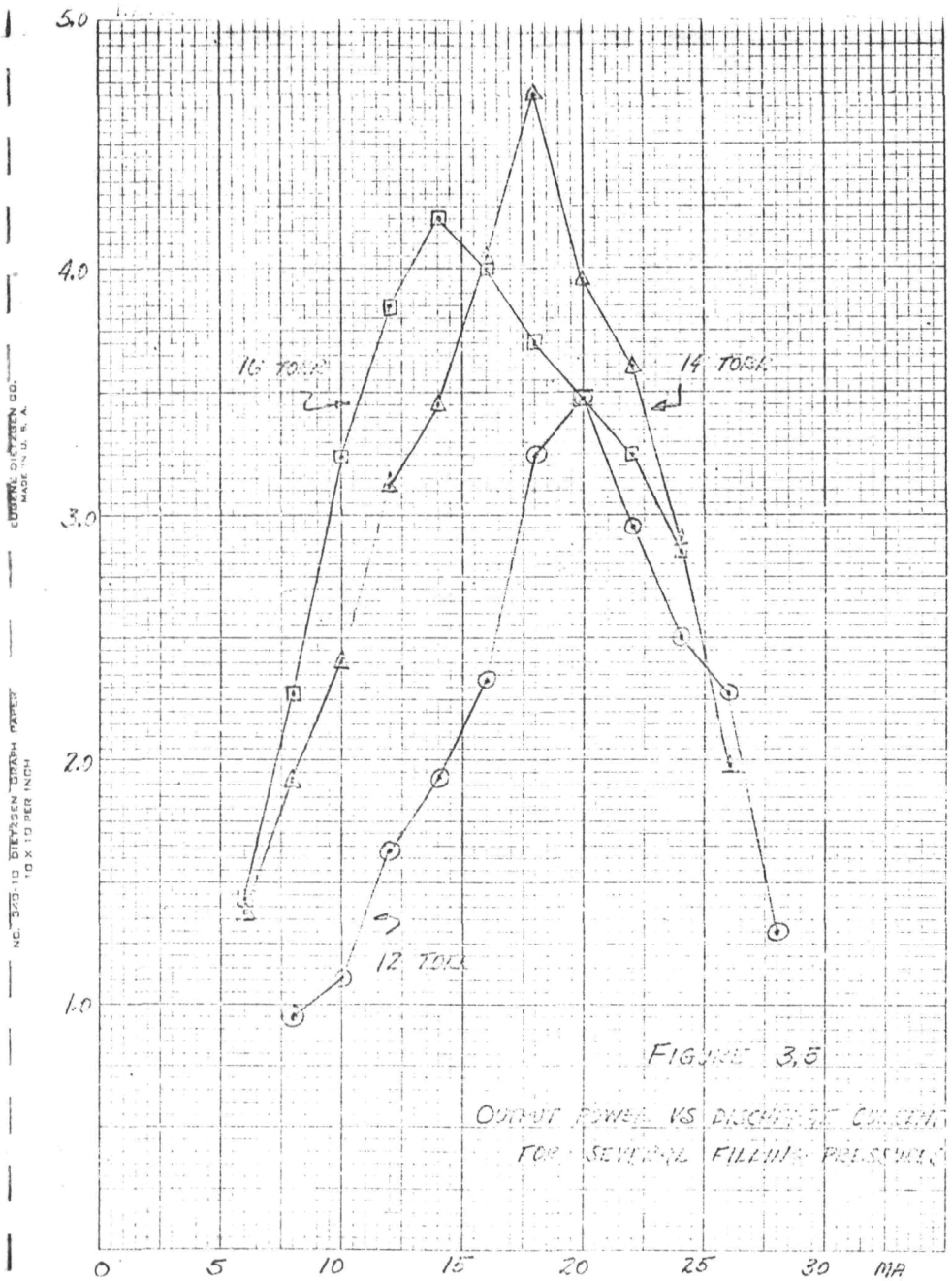

FIGURE 3.5

OUTPUT POWER VS DISCHARGE CURRENT FOR SEVERAL FILLING PRESSURES

This general deterioration of laser operating performance could be attributed to several factors. There is undoubtedly some contamination of the discharge due to sputtering from the neon sign electrodes. There also has been a general deterioration of the quality of the front Irtran window. Upon occasion it has been observed that the discharge would arc to it and thereby affect the aluminized coating. Also, in a laser of only one-meter discharge length, the optical quality of the Brewster-angle window is of greater importance than with longer lasers. Although this window has been kept in a heated atmosphere throughout its life, there has been a gradual deterioration and fogging of the sodium chloride. In recent experiments, the laser as originally constructed has failed to operate using the pre-mixed gas mixture. Operation at power levels up to three watts could only be achieved through the careful addition of CO_2 and He to the pre-mixed gas. In general, recent operation was best achieved at considerably lower pressures, namely 8 - 10 torr, than the 14 torr used in the earliest experiments. Unfortunately there were not sufficient funds available to allow refurbishing and replacement of the deteriorated optical components.

At almost any given time, the laser will operate at a relatively constant output powers over periods of up to several days. Output power was generally more uniform when the laser was operating in a multimode configuration. Single mode operation in the TEM 00 mode could be achieved readily using an adjustable diaphragm near the rear mirror location and reducing the aperture to eliminate off-axis modes. Output power, however, was reduced by 50%. When operating in a single mode configuration there were somewhat greater variations in output power level. These were primarily due to thermal expansion and contraction of the laser cavity.

As might be expected these variations were considerably more pronounced when the laser was operated at a single wavelength using the diffraction grating. This will be discussed further below. Figure 3-6 shows multimode output level variation as monitored over an approximately two-hour period using the Coherent Radiation Laboratory power meter. The chart recorder does not respond to the many rapid variations in output power.

Wavelength Shifting Experiments:

As proposed in the work of Hanst[15,16], the method by which laser wavelength tuning can be accomplished through an intracavity absorption gas was tried. In these experiments a gas cell was fitted into the laser optical cavity. The cell was roughly 10 cm long with a Brewster's-angle sodium chloride window at one end while the other end was made vacuum-tight against the ground glass tapered joint on the rear end of the laser itself. Using a Beckman IR-2 Spectrophotometer the laser output wavelength was monitored as a function of pressure using propylene for the wavelength-shifting gas. Figure 3.7 shows the variation of laser wavelength with absorption cell pressures.

Over the range of pressures employed lasing action was observed in all four possible regions, that is, both P and R branches of the $00^{o}1$ - $10^{o}0$ and $00^{o}1$ - $2^{o}0$ bands. Often lasing would occur in three regions simultaneously, for instance 9.3, 9.6 and 10.6 microns. Except for the anticipated result that the lasing shifts to shorter wavelengths with higher propylene pressure, the wavelength selection could not be termed reproducible in the sense of being able to assign a definite (and exclusive) operating wavelength to a given gas cell pressure.

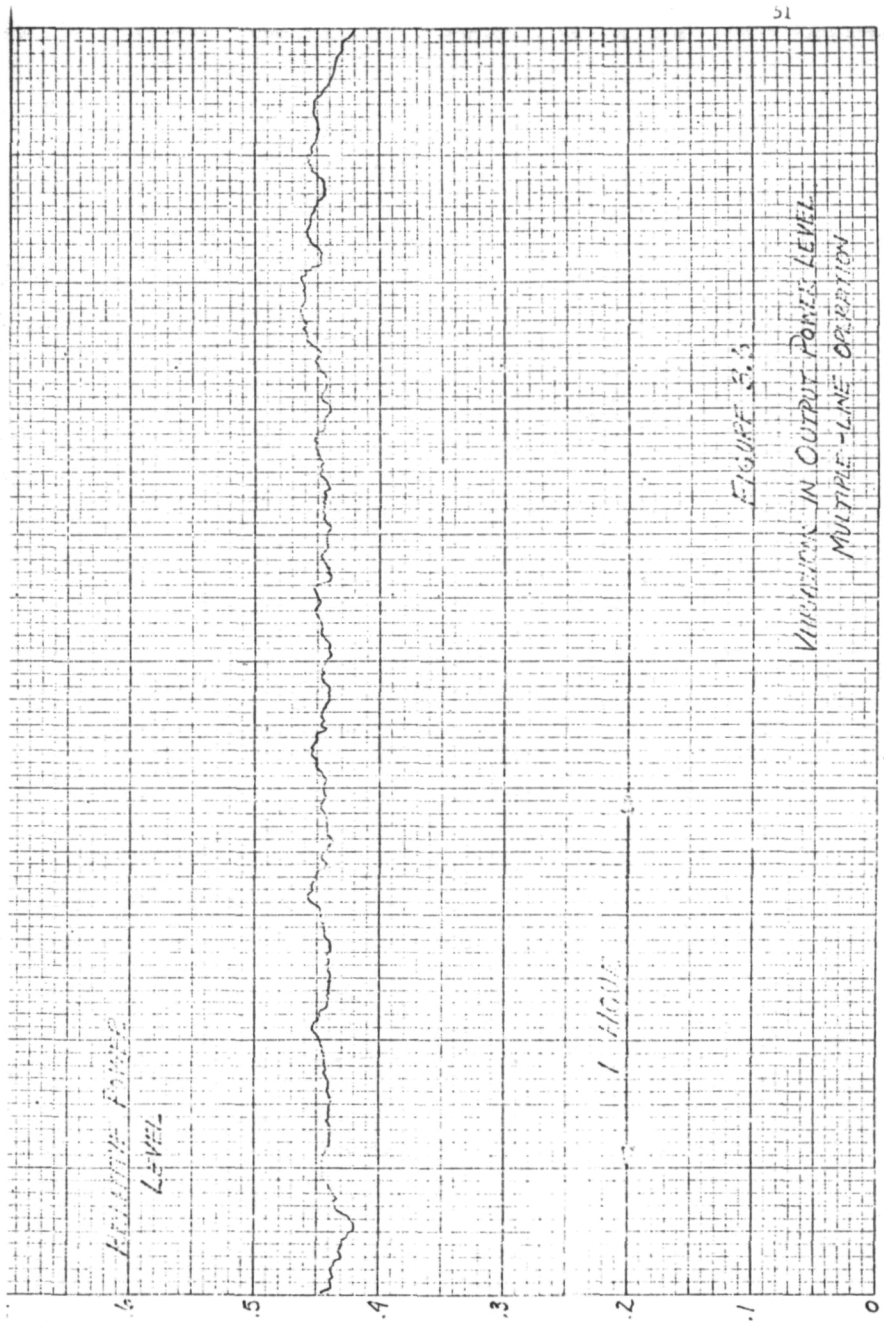

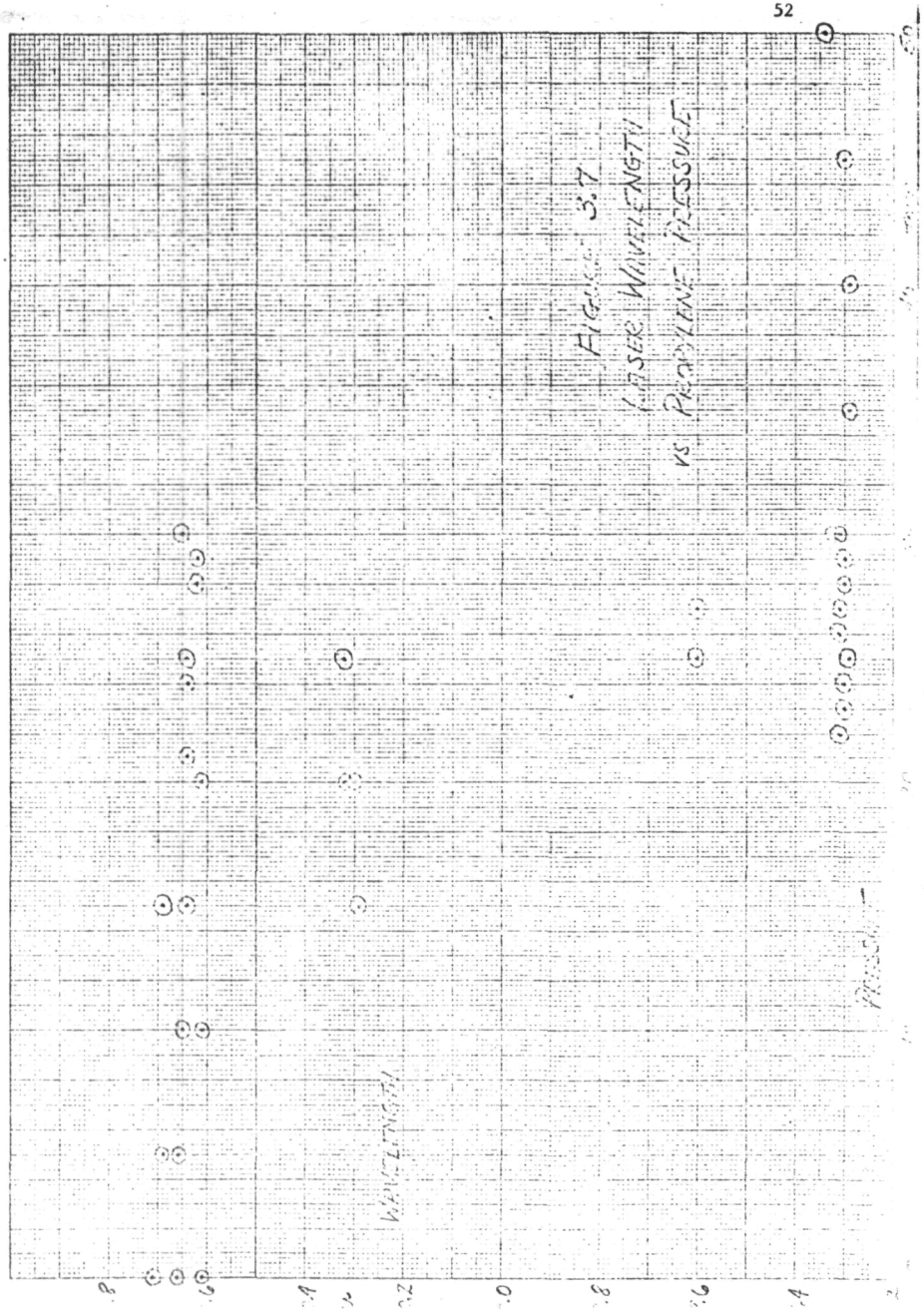

For use as an air pollution monitoring tool, such operation on multiple wavelengths is clearly unsuitable where molecular absorption must be studied. Also the output power was reduced considerably, to 10% of normal, when 30 or 40 torr of propylene was added to the cell. After several experiments had produced substantially the same results, it was decided to abandon the absorption-cell technique in favor of using the intracavity-diffraction grating. A further factor in this decision was that the absorption cell required additional gas-handling apparatus and would particularly complicate field operation.

For the diffraction grating experiments, an inexpensive grating was obtained from the Ealing Corporation. The grating measures 1 X 1¼ inches and contains 1500 lines per inch or 57 lines per mm and is blazed for 11 microns. At first the grating replaced the gold-coated spherical reflector in the rear of the laser cavity. The grating is normally aluminized and will operate in the laser in that condition. However, improved results were obtained by over-coating the grating with a thin layer of approximately 100Å thick of vapor-deposited gold. In this condition up to about 1 watt of output power was obtained on the highest gain laser line by careful grating adjustment and optimization of the gas filling mixture. The grating was mounted in a Lansing Gimballed mount and after several calibration trials, various laser wavelengths could be selected at will through the use of the micrometer dial. These settings were found to be repeatable and could allow for easy wavelength selection in the field. It is important that single wavelength operation must be accompanied by extremely stable mechanical configuration to ensure stable output powers.

Figure 3-8 shows the wavelengths and their relative output powers obtained through micrometer adjustment of the diffraction grating. The wavelength figures are approximate and represent the maximum accuracy of the Beckman-prism-spectrometer. The output powers roughly approximate the expected gain profile for the various output lines.

The particular wavelengths quoted in reference 16 as being the optimum wavelength for monitoring ethylene pollution does not exist in these CO_2 laser spectra. Indeed the particular line mentioned of 10.528 microns does not correspond to any published CO_2 line nor is it theoretically postulated. The only two lines in this wavelength's region are at 10.513 and 10.532 microns corresponding to the P(12) and P(14) transitions respectively.

As a function of time the output from the single wavelength laser showed marked variations with time, beginning with initial turn-on and continuing for several hours. After this time, as shown in Figure 3-9, the output power was considerably more uniform and was primarily due to thermal stabilization of the laser and its optical cavity. Part of the problem of having an internal window laser is that the optical cavity is dependent upon the heat-producing element itself, namely the laser discharge tube. Thus gross thermal distortions occur as the laser discharge is operated. A preferable arrangement is to have all elements of the optical cavity thermally isolated from the heat-producing discharge tube.

When using the grating the laser cavity essentially consisted of two flat mirrors and was thus only marginally stable. With adjustment the output could be obtained in the lowest order mode, that is TEM 00, although with time thermal distortions would lead to higher order modes.

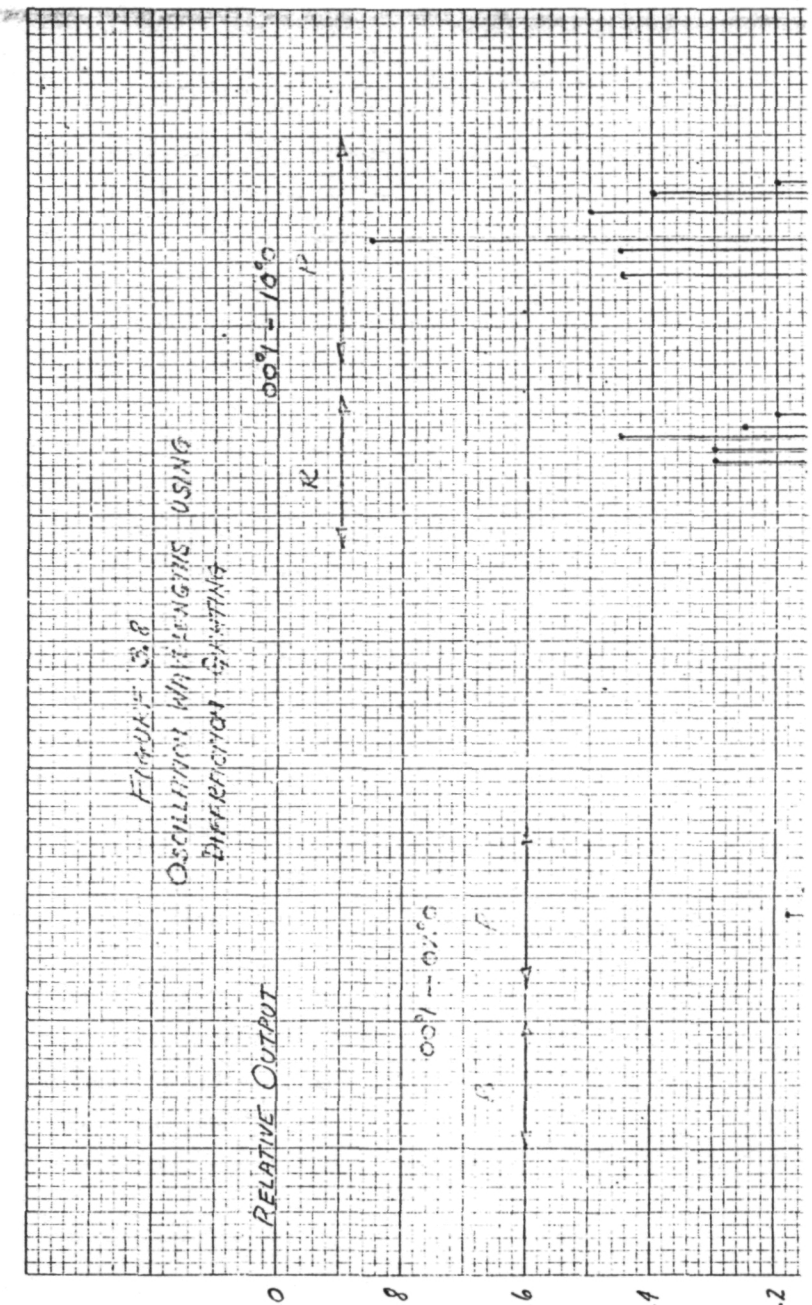

Page Intentionally Left Blank

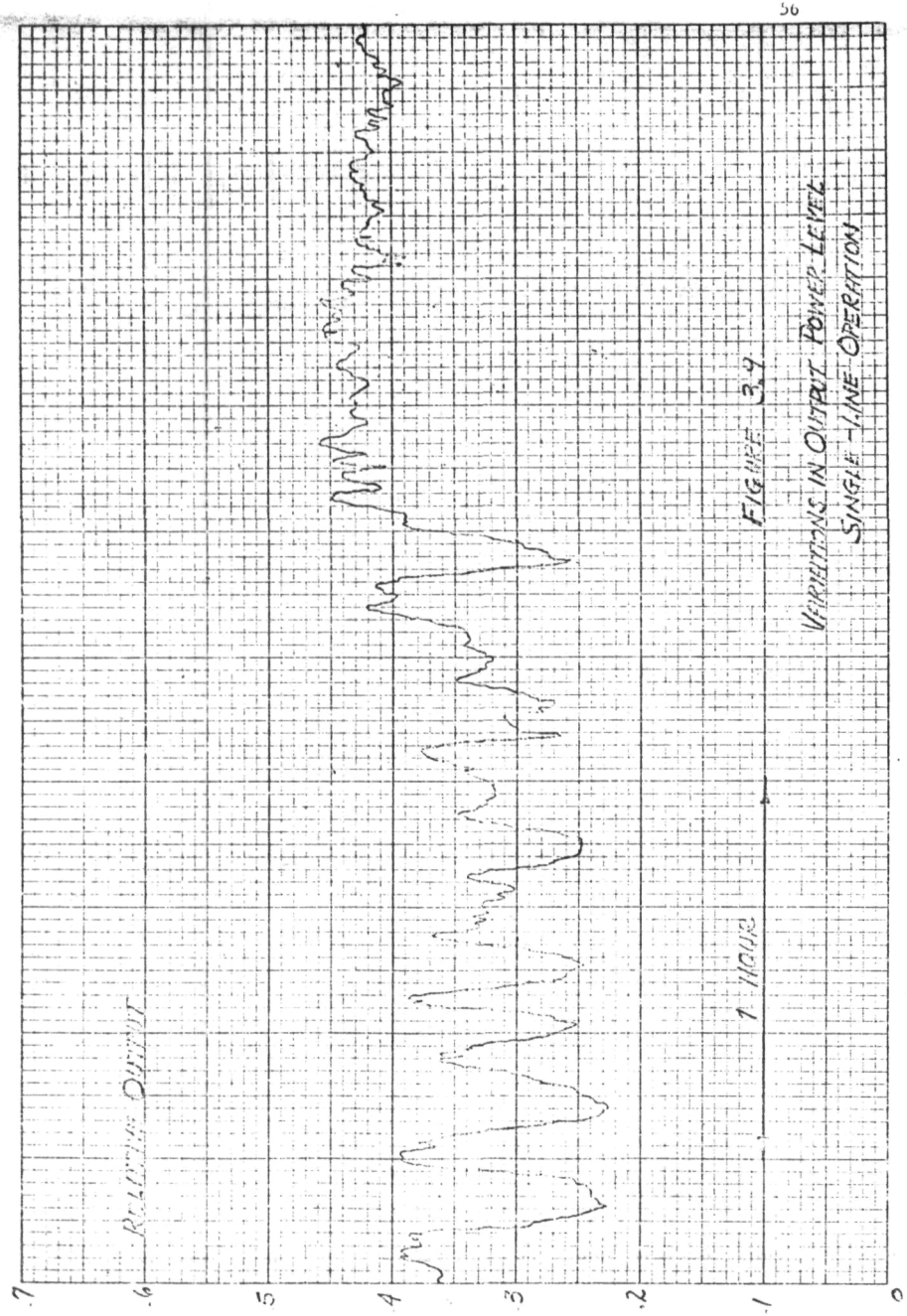

FIGURE 3-9
VARIATIONS IN OUTPUT POWER LEVEL
SINGLE-LINE OPERATION

In any realistic air pollution monitoring system, it is important that both lasers be "mode stable" because the amount of energy reflected from the target will be dependent upon the beam divergence which is a function of the laser operating mode. Although two diffraction gratings were ordered originally, the second unit was not received until after the completion date of the contract and thus a second tuneable laser was not assembled.

DETAILS of RECEIVING SYSTEM

Optics and Detector:

The receiver optical system consists of an 8-inch diameter Newtonian astronomical telescope modified for use with infrared detectors and circuitry. The telescope was obtained from the Edmund Scientific Company complete with a heavy duty pedestal mount and a suitable adjustment mechanism. In this unit, the primary mirror is a 64-inch F-8 aluminized spherical mirror. The secondary mirror is eliptical and mounted on axis at 45^{o} angle of incidence. This mirror serves to reflect the image outside of the field of view of the telescope. A two-axis adjustable mount was fabricated and placed at the focal point to accommodate the gold-doped germanium infrared detector and its associated components. An additional mirror on a rotating mount is employed here so that in one position the telescope image is focussed on the infrared detector and in the second position the image can be focussed either for visual observation or for use by a different detector. The complete detector assembly is shown in Figure 3-10.

The infrared detector employed is a Philco GPC-216A gold-doped germanium unit. It operates at liquid N_2 temperature of 77^{o} Kelvin and can be cooled either by liquid N_2 filling or a high pressure N_2 cryostat.

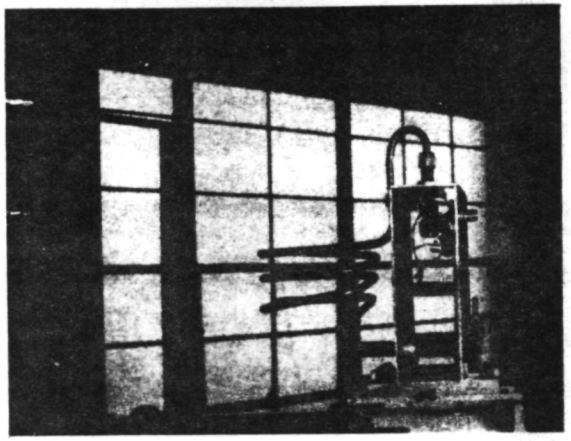

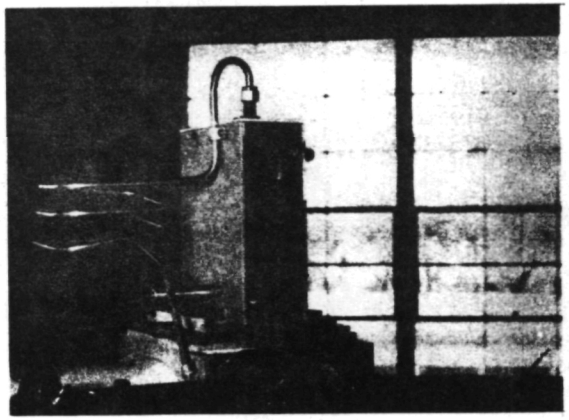

FIGURE 3-10. Mount and Housing for Germanium Infrared Detector.

Although our experience when using the cryostat has not been entirely satisfactory, it is felt that this method is superior to the use of liquid N_2 particularly for field operation. The fine orifice of the cryostat requires that the gas be of exceptionally high purity and very dry, for the slightest moisture in the gas will freeze and clog the cryostat, resulting in a loss of cooling power. The commercially available dry N_2 must be passed through a chemical drying filter in order to completely eliminate the remanent water vapor. Depending on the inlet pressure up to three or four minutes are required to cool the detector initially. Besides being less awkward to use, the cryostat also eliminates the possibility of thermal shock to the detector window by liquid N_2 spillage. Such spillage may completely fracture barium-flouride window and lead to further detector breakage.

The bias circuitry and load resistor for the detector are incorporated in its housing situated on the telescope. Provision was not made to include a cooled infrared filter ahead of this detector because it was felt the signal-to-noise ratio presently obtainable did not warrant the additional complication.

The manufacturers test data for this particular detector indicate a detectivity D* of 2.76×10^9 cm $H_Z^{\frac{1}{2}}$ per watt for a 500°K black body (emission peak $\sim$ 5.5 microns at 500°K). Under the test conditions this figure corresponds to a responsivity R of 3200 volts per watt at 40 μa bias. Spectral response curves typically indicate this figure should be decreased by greater than a factor of ten at 10.6 microns.

To check the overall receiver responsivity under operating conditions the test arrangement shown in Figure 3-11 was used. Each of the two sodium chloride beam splitters reflects an average of 1.66% of the laser beam at 45^o incidence.

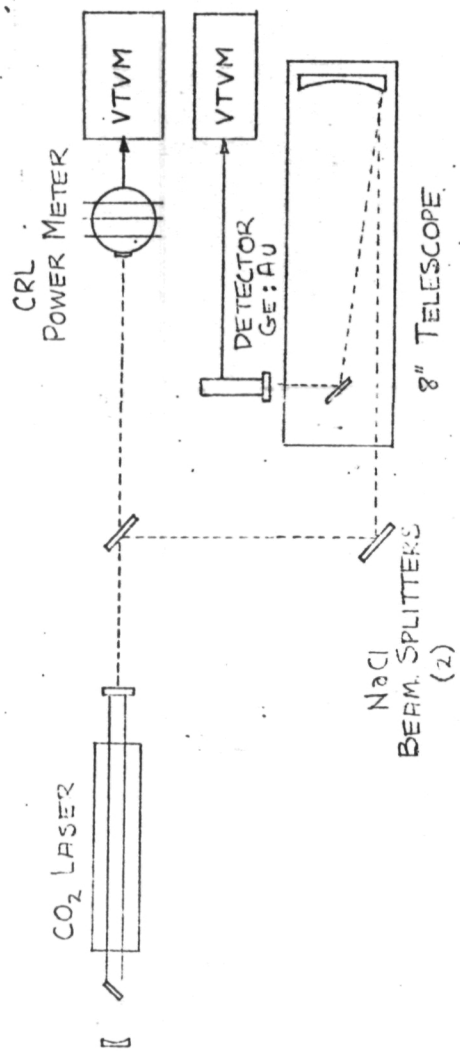

FIGURE 3.11
CALIBRATION OF GERMANIUM DETECTOR

The power level at the detector is thus 2.76 X 10^{-4} of the laser output power. It is actually slightly less after undergoing the two additional mirror reflections. Data taken of the detector signal response to various laser output powers indicate an overall responsivity of approximately 150 volts per watt at 10.6 microns. This value is reasonable in view of the approximate nature of the spectral data mentioned above.

Transmitter-Receiver Assembly:

The original telescope mounting frame was fitted with side extensions so that the two laser-transmitter assemblies could be mounted on either side of the telescope. The lasers are individually adjustable over a small range of azimuth and elevation for boresighting. The entire assembly, as shown in Figure 3-12, weighs about 200 pounds. Included on the mount are the excitation transformers, water manifold, and high pressure plumbing for the cryostat.

The mount is adjustable in azimuth and elevation for the selection of various retroreflector stations. Alignment is most readily accomplished by flipping the moveable detector mirror to permit visual sighting and centering of the telescope image. This is considerably simplified with the aid of a small He-Ne laser to provide a visible return beam from the retroreflector. The mirror is flipped back to its original position and the telescope image is then in focus on the sensitive detector area.

Signal Processing Electronics:

The most ideal situation from the point of view of real time signal processing would be to have two separate lock-in amplifiers fed in parallel from the output of the infrared detector.

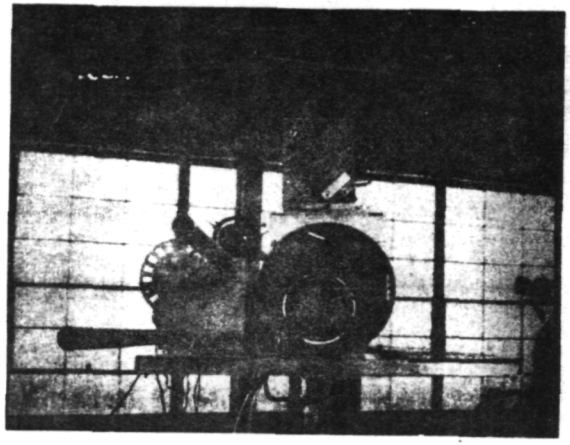

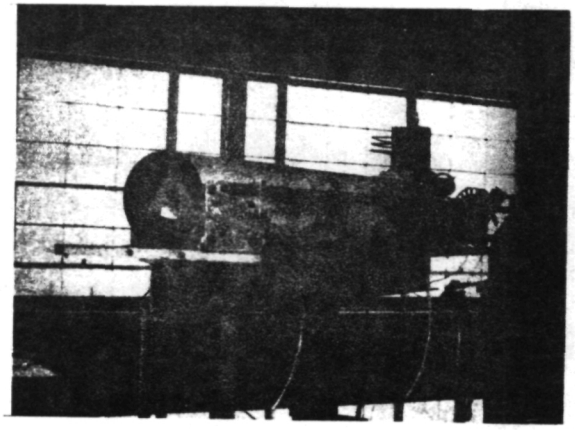

FIGURE 3-12. Overall Views of Receiver-Transmitter.

Each amplifier would be referenced to the particular chopping frequency of its associated laser. By comparing the laser output level as measured on the thermistor with the received signal detected by the lock-in amplifier, the overall attenuation of that laser beam would be obtained.

One possible implementation of such a system is as shown in Figure 3-13. The output power monitor signals are synchronously rectified and together with the appropriate received laser signal fed to operational analog dividers to form the normalized received/transmitted ratio. Inexpensive division networks employing the Motorola MC-1335 analog multiplier may be used. A third ratio circuit computes the relative attenuation of the two beams which is a function of pollutant concentration.

However, as funds were insufficient in this contract to include the purchase of the necessary two lock-in amplifiers, an alternative arrangement has been worked out and found satisfactory for trial runs. As diagrammed in Figure 3-14, the infrared detector output is amplified by a low-noise adjustable band-width amplifier and recorded directly on instrumentation-grade FM tape recorder. Likewise the reference signal outputs from the two beam choppers and the output power monitoring signals are also recorded simultaneously. Thus at a subsequent time a single lock-in amplifier can be connected to the various channels of the FM recorder and synchronized to one or the other reference frequency as desired. While this method does not yield results in real time, it is suitable for the experimentation which has been in process. It is proposed that future work in this area will permit acquisition of the necessary additional electronics to permit real time continuous absorption monitoring.

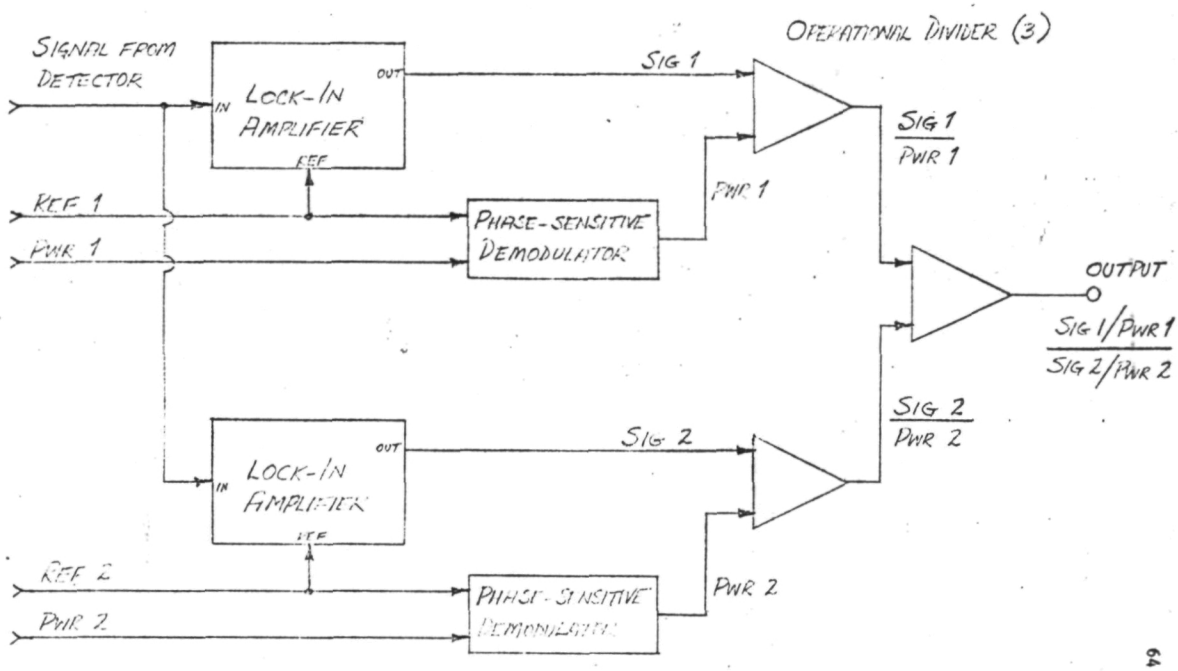

FIGURE 3.13 PROPOSED ELECTRONIC SIGNAL PROCESSING SCHEME

64

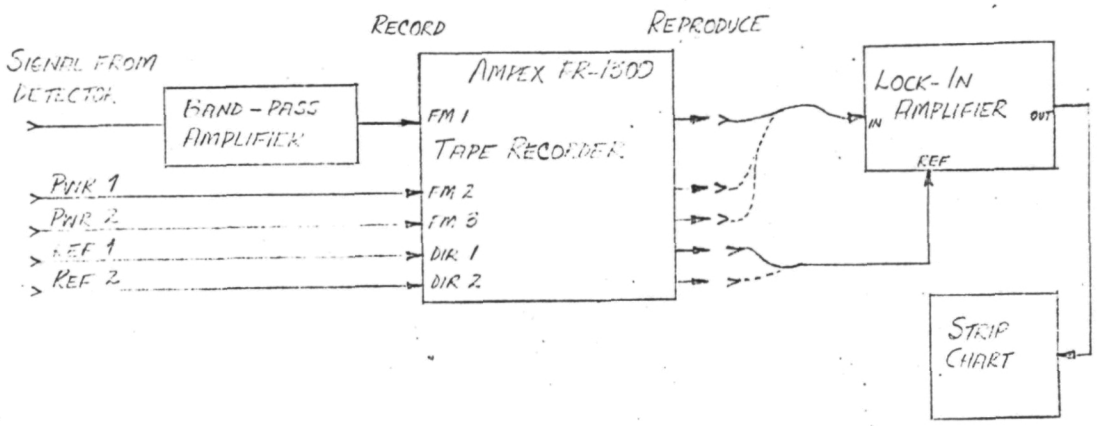

FIGURE 3.14 CURRENT ELECTRONIC SIGNAL PROCESSING SYSTEM

65

RETROREFLECTORS

Two retroreflector mirror stations have been established in line-of-sight from the laboratory transmitter/receiver location. In each case, the retroreflector station consists of a two-inch diameter hollow-corner cube prism which had been first surfaced gold-coated. These prisms were obtained from the Electro-Optical Systems Company. The prisms are mounted in the extreme rear end of an exponential type horn which as shown in Figure 3-15, mainly provides weather protection. The stations are located at 700 and 1650 feet respectively from the transmitting site, giving two-way paths of 1400 and 3300 feet respectively. As the two-inch diameter of these retroreflectors is considered rather small for the long paths ultimately envisioned (5000 feet) some plans have been made for the construction of larger units. At their present price it is uneconomical to consider clustering these small units in multiples such as 9. However, with the aid of accurate rotary mill table, a mechanical assembly is anticipated which will hold three individual first surface mirrors with the required accuracy. Assemblies having mirrors up to six inches square are currently under consideration. These would provide significant improvement in the returned signal level and consequently greater measurement accuracy.

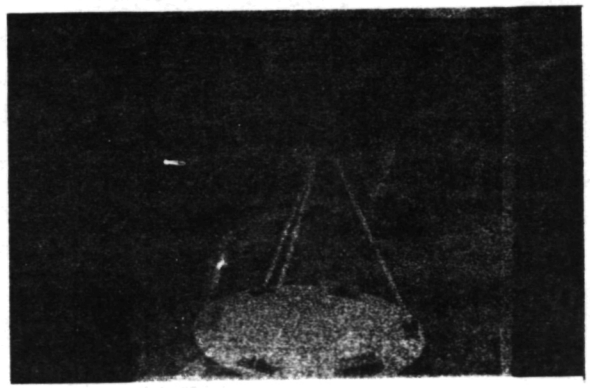

FIGURE 3-15. Remote Retroreflector on Tripod Mounting.

CHAPTER IV

EXPERIMENTAL MEASUREMENTS and OBSERVATIONS

Having assembled the basic hardware components and observed their characteristics and limitations a number transmission/reception experiments were performed to gain experience with the system and monitor its performance. As discussed later several problems prevented the realization of the complete two-laser system. However, the experience gained when operating with a single laser has proven most valuable and will doubtless result in significant improvements for future operation.

SHORT and LONG PATH RECEPTION EXPERIMENTS

Using a single laser the received signal characteristics from both the short- and long-path retroreflectors were observed on numerous occasions. It was found mandatory to first align the receiver optical system using a He-Ne laser and position the pedestal mount to obtain the strongest visible return in the sighting eyepiece of the telescope. By re-adjusting the moveable mirror the focussed red image could be directed onto the germanium detector and centered in the sensitive region.

The cryostat was then pressurized to 1800 psi. Detector temperature as it cooled was monitored by observing the bias current. A bias current of 80 microamperes at room temperature decreased to 40 microamperes as the detector cooled to 77°K. Cooling time was 1 - 2 minutes. Next the beam choppers were energized and the lock-in amplifier synchronized to the chopper reference signal. With the receiving system readied the laser was excited and carefully boresighted until the maximum return signal was observed. The laser was locked in that position.

For an output power level of approximately one watt, the received signal level indicated on the lock-in amplifier, for both long- and short-path operation, was in the range 500 - 1000 microvolts. The maximum observed signal was 1.8 mv on the short-path. With the detector responsivity measured to be 150 volts per watt, this signal level range corresponds to a received power of 3-6 X 10^{-6} watts. The path loss is therefore roughly 55 db. No reliable difference could be defined in the path losses for the two paths, primarily because of the rapid and random received signal fluctuations. It was also difficult to ascertain whether or not a given alignment was optimum. When operating at these distances the sensitivity of the system to mechanical motion is severe, and it is difficult to improve an adjustment without greatly disturbing the status quo.

With the laser on, but the beam blocked, the measured noise at 1200 cps was 3 microvolts or less. Thus even with a very modest laser output and using no infrared filters, a net signal-to-noise ratio in excess of 200:1 was generally obtained. When using ordinary AC excitation, the laser output is 100% amplitude modulated at 120 cps. It is possible to synchronize the lock-in amplifier to this frequency (the chopper is turned off) and observe the received signal. A maximum signal of five millivolts was obtained on the long path (laser output ∿ .75 watt). The noise was also somewhat higher, 10 - 15 microvolts, because of the gas discharge and the signal-to-noise ratio thus remained almost the same. The signal-to-noise ratio can be expected to be somewhat higher when using DC excitation.

During one lengthy continuous monitoring experiment both the output from the laser power monitor and the output from the detector amplifier were recorded on the FM tape recorder.

As described in Chapter III these two signals could be played back one at a time into the lock-in amplifier and recorded on a strip chart. Typical results showing the laser output and the corresponding received signal are shown in Figure 4-1. Although the received signal shows much more variance than the transmitted signal, it appears their average ratio remains nearly constant. To exactly what level of precision it is a constant has not yet been determined. The graph in Figure 4-2 shows the received signal as the laser excitation is varied from zero to full several times.

With regard to the constancy of the received/transmitted signal ratio it is quite important that the laser be mode stable. It has been observed that through mechanical or thermal effects the laser mode pattern can shift without greatly affecting the output power level. However the beam divergence and energy distribution both change significantly and therefore does the power returned by the retroreflector.

As might be expected, the pointing accuracy requirements when operating over a 1650 foot pathway are severe, and small mechanical vibrations, distortions, or other misalignments can greatly affect the received signal level. Walking near the transmitter/receiver produced a noticeable effect. Two factors contributing to this sensitivity are 1) the small angular divergence of the laser beam, and 2) the small field of view of the telescope operating with the .01 cm^2 detector at its focus. In the present system both of these angular tolerances are roughly the same, approximately .5 milliradian. A pointing deviation of about .25 milliradian, therefore, will virtually eliminate the return signal.

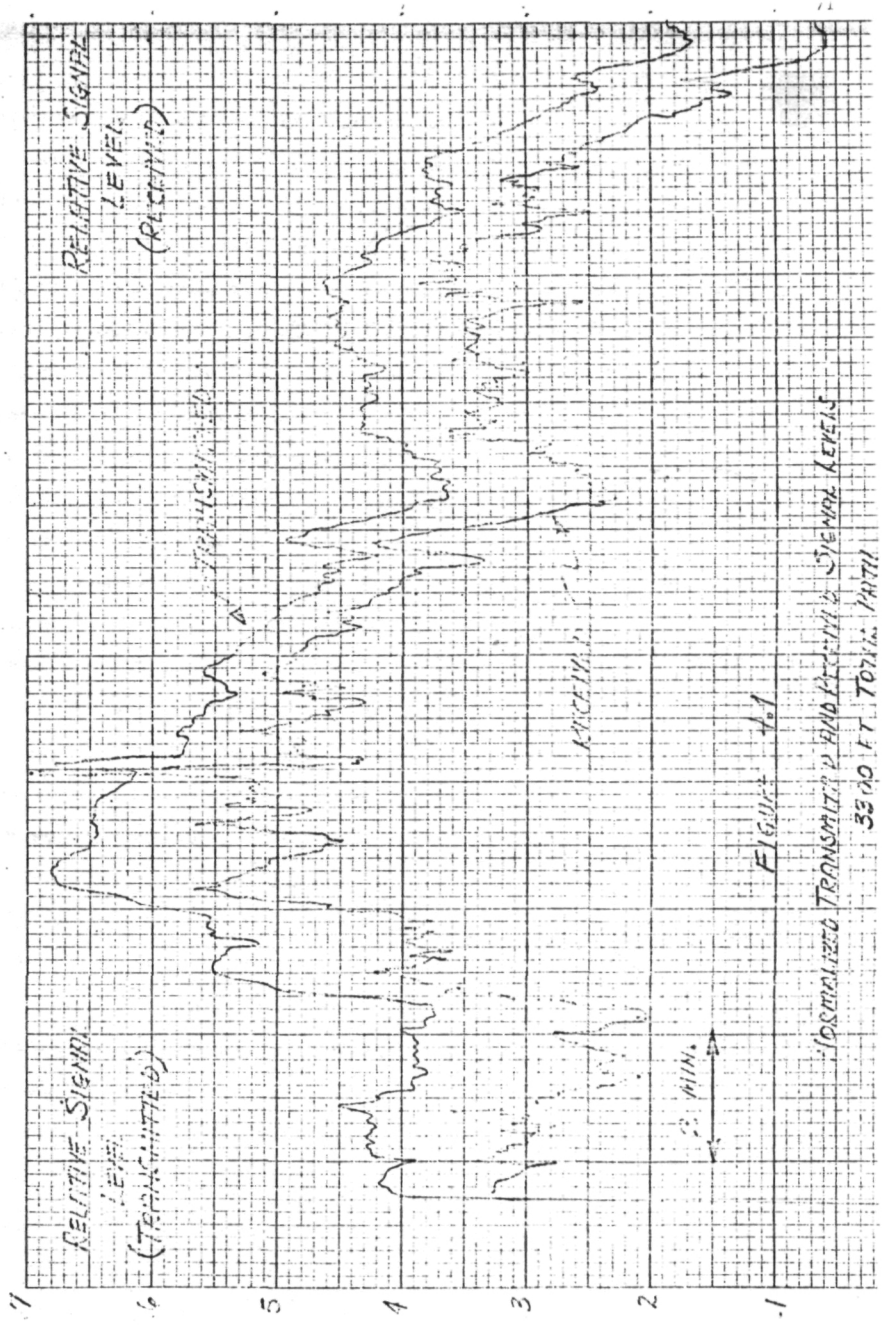

Page Intentionally Left Blank

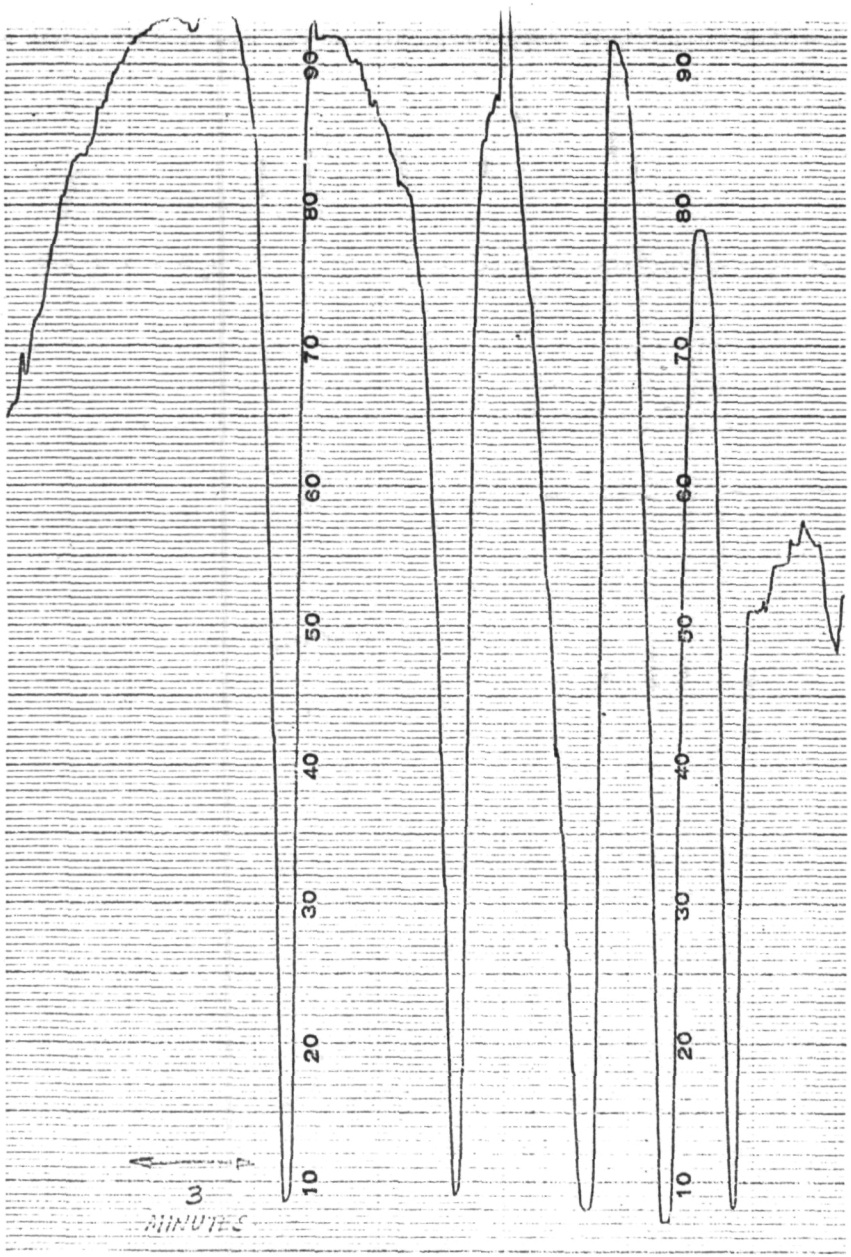

FIGURE 4-2(a). Normalized Transmitter Output Power, Manually Cycled.

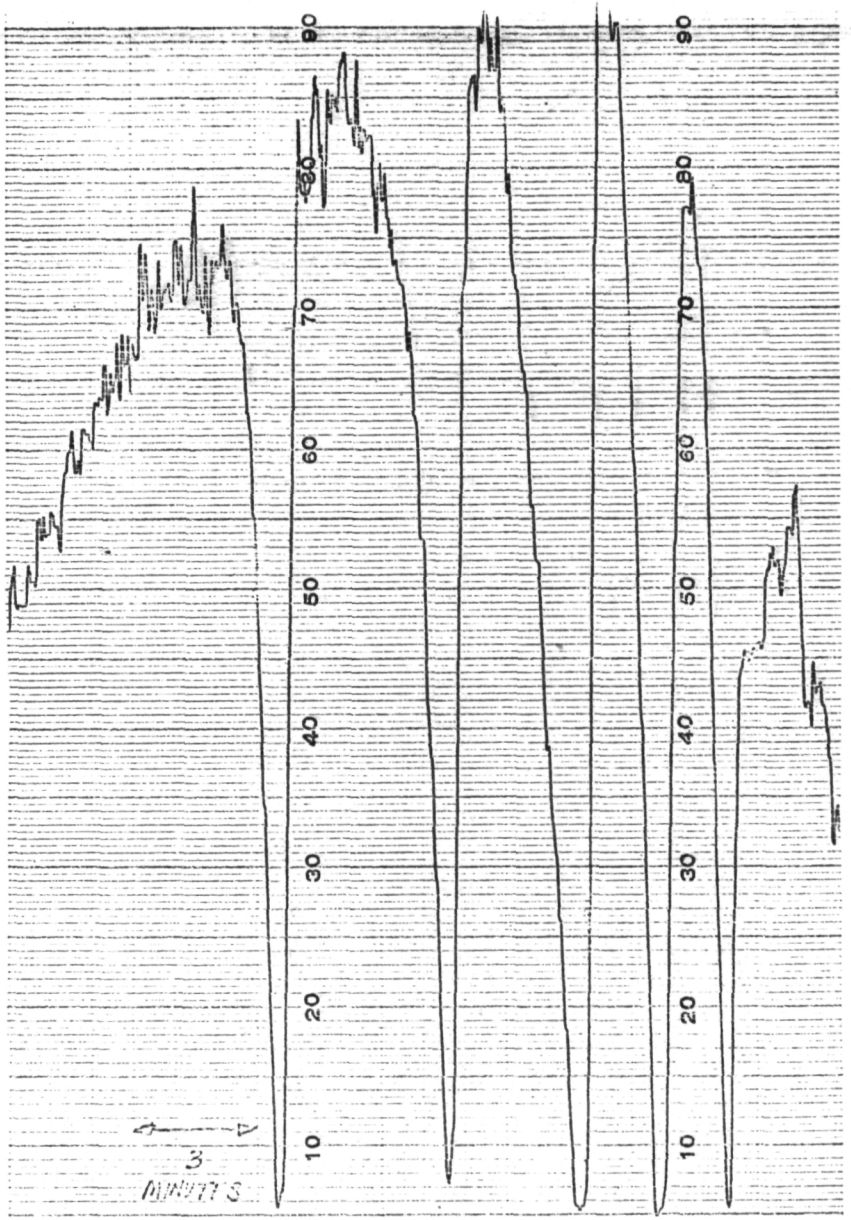

FIGURE 4-2(b). Normalized Received Signal Corresponding to Figure 4-2(a); 3300-foot Path.

PROBLEMS ENCOUNTERED in OPERATION

Throughout the duration of the contract, trouble was continually experienced with laser reliability. In general, it was not possible to maintain two operating lasers concurrently. A variety of difficulties were encountered, many of which appeared to be fundamental to the particular design and implementation of the laser devices themselves.

Pinhole leaks in the glass laser tube and the surrounding reservoir presented difficulties.

Use of the spherical glass joint for the front window pivot poses a problem with regard to the front mirror adjustment. It is imperative in any laser which is to be wavelength stable that the mirror adjustments must be precise and free of mechanical and thermal distortion. Internal mirror lasers suffer in that the optical cavity is coupled to the major heat producing element, that is, the discharge tube. It is felt that a laser tube with two Brewster-angle windows and external mirrors would prove much easier to adjust and maintain. A second problem involving the internal front window arises when the DC or AC discharge arcs to the aluminized coating of the front reflector. This is particularly possible in cases where the front window adjustment operates on the window itself. An alternative mechanism places a metal collar around the pivoting glass tube, about 1 cm from the end window. Adjustment screws then operate against the collar. Arcing to the aluminized window surface can only result in a deterioration of the highly reflecting coating.

The use of Apiezon - W wax as a front window seal also is not to be recommended. At the higher power levels attainable there is sufficient absorption in the Irtran II window to heat it to a sufficient temperature that the wax melts. A vacuum grade epoxy such as torr-seal has been found satisfactory.

A problem which has consistently plagued laser operation has been melting of the glass in the electrode arms. This has been observed to occur at even very modest input power levels. The problem arises because the tubular glass electrode arms are radiused 90^{o} before joining the main discharge tube. The outside wall of the radius is made too thin to accommodate the heat dissipated by the discharge near the electrodes. Consequently, while operating, a pinhole leak often developes. This interrupts laser operation immediately and without prior warning. Two solutions which are recommended for this problem include, first, the use of heavier glass tubing in making the electrode arms and, secondly, the addition of heat dissipating radiators attached to the electrodes to keep them cooler. A third recommendation would be to extend the water jacket closer to the electrode arms or perhaps include some means for water cooling the electrodes themselves.

Considerable difficulty has been experienced at the rear Brewster-angle window. Here, without prior indication, the glass of the discharge tube will suddenly shatter or fracture and immediately spoil the vacuum.

In some cases the sodium chloride window will also fracture. We have used windows cemented with both epoxy and Silastic silicon rubber and have experienced similar fractures. It outwardly appears to be a thermal problem; however, it could also be related to unrelieved strains in the laser tube after it is cut.

A further problem which has caused some breakages has been the very fragile manner in which the stopcocks were attached to the main laser tube. It is felt that a larger diameter stopcock would be considerably stronger than the small bore units now being used.

In summary we would recommend the following type of laser configuration for the reliable operation that is required in this project. The laser should have two Brewster-angle windows with external mirrors. The electrode arms should be heavy-walled glass tubing and should have provision for water cooling or forced air cooling. In addition heat dissipation radiators should be attached to the electrodes. Larger stopcocks would allow for less breakage.

Recent published data indicate that the large volume gas reservoir is not necessary if: 1) the electrodes are made of a non-sputtering, non-reacting material such as platinum, 2) the discharge tube can be baked out to remove adsorbed impurities, 3) the filling gases are pure and with a small amount of water vapor added to the mixture. Lifetimes of several thousand hours are reported. (17,18,19) Unfortunately there were not sufficient funds included in the contract to permit the redesign and construction of the new lasers as necessary. As of this writing, of the three lasers originally ordered, only one is operational and it has been extensively reworked and repatched.

Finally, after some eight months of continuous weather exposure, the gold-coated reflector at the short-path station showed numerous signs of corrosion and gold flaking. In fact, the returned signal from a He-Ne laser was less at the 700-foot distance than the signal obtained from the 1650-foot station. Presumably, however, deterioration of the reflector quality would only decrease the signal-to-noise ratio and would not lead to any differential absorption error in a dual-beam laser system.

CHAPTER V

SUMMARY and CONCLUSIONS

The basic items of the project year have been met with some exceptions.

The equipment has been installed and is partly operational. Two folded optical paths of 1400 feet and 3300 feet total length have been established and the LASER transmissions have been tested over these paths. The longest path is less than the planned 10,000 foot path and this shortcoming was due directly to an inordinate number of unexpected hardware problems. The full checks with chemical techniques and comparisons with weather patterns were similarly curtailed.

There were other conclusions derived from this year's effort.

The power capabilities of this size LASER seems to be adequate for longer paths, possibly several miles. It is not known how rapidly the scintillation effect will increase and therefore optimum and maximum path lengths are not known.

It is certain that more emphasis will be required on LASER and reflector mount stability for longer paths.

The present LASER configuration will have to be modified for greater mechanical strength, reliability, and stability for any protracted application.

The present design of gold-plated retroreflectors will require some modification by reason of observed weathering effects.

In projection, mathematical analysis has shown that the potential of this probe-type application has significant potential as an area survey or monitoring system. In concert, multiple paths could be used for the evaluation of range and direction of polluting sources from the local area.

While a few of the results have dramatized some problems, it is apparent that the application of LASER methodology to atmospheric mensuration is a definite probability. The final evaluation must come from further development and larger scale application.

LIST of REFERENCES

1. Hanst, P.L. et al, "Absorptivities for the Infrared Determination of Trace Amounts of Ozone", Analytical Chemistry, 33, 1113 (1961).

2. Pierson, R. H. et al, "Catalog of Infrared Spectra for the Qualitative Analysis of Gases", Analytical Chemistry 28, 1218 (1956).

3. Long, R. K. "Atmospheric Absorption and Laser Radiation" Bulletin 199 Eng. Exp Station, Ohio State University, (1967).

4. D. L. Fried, G. E. Mevers and M. P. Keister, Jr., "Measurements of Laser-Beam Scintillation in the Atmosphere", J. Opt. Soc. Am., Vol. 57, pp. 787-797, June (1967).

5. D. H. Höhn, "Effects of Atmospheric Turbulence on the Transmission of a Laser Beam at 6328 Å. I-Distribution of Intensity; II-Frequency Spectra", Appl. Opt., Vol. 5, pp. 1427-1436, Sept. (1966).

6. M. W. Fitzmaurice, J. L. Bufton and P. O. Minott, "Wavelength Dependence of Laser-Beam Scintillation", J. Opt. Soc. Am., Vol. 57, pp. 7-10, Jan. (1969).

7. V. I. Tatarski, "Wave Propagation in a Turbulent Medium", McGraw-Hill Book Co. New York, (1961).

8. A. L. Buck, "Effects of the Atmosphere on Laser Beam Propagation", Appl. Opt., Vol. 6, pp. 703-708, Apr. (1967).

9. P. H. Deltz and N. J. Wright, "Saturation of Scintillation Magnitude in Near-Earth Optical Propagation", Ballistic Research Labs, Aberdeen Proving Ground, Md., Rept BRL-MR-1941-Rev., Oct. (1968).

10. R. D. Rosner, "Hetrodyne Detection of an Optical Signal After One-Way Propagation on an Atmospheric Path", Proc. IEEE (letters), Vol. 56 pp. 126-128, Jan. (1968).

11. R. F. Lucy and K. Lang, "Optical Communications Experiments at 6328 Å and 10.6 μ," Appl. Opt. Vol. 7, pp. 1965-1970, Oct. (1968).

12. Stern, A. C., ed, "Air Pollution", Vol. I, Academic Press, New York, London (1968).

13. Hansen, F. V., "Predicting Diffusion of Atmospheric Contaminants by Consideration of Turbulent Characteristics of WSMR", ECOM-5170 atmospheric Sciences Lab. White Sands Missile Range, New Mexico, Jan. (1968).

14. Sutton, O. G. "Micrometeorology", McGraw-Hill, New York and London. (1953).

15. Hanst, P. L. and Morreal, J. A. "A Wavelength-Selective, Repetitively Pulsed CO_2 Laser". Appl Opt. 8, 109 (1969).

16. Hanst, P. L. and Morreal, J. A. "Detection and Measurement of Air Pollutants by Absorption of Infrared Laser Radiation", Air Pollution Control Association Meeting, June (1968).

17. Witteman, W. J. "High Output Powers and Long Lifetimes of Sealed-Off CO_2 Lasers", Appl. Phys Lett 11, 337 (1967).

18. Witteman, W. J., "Increasing Continuous Laser Action on CO_2 Rotational-Vibrational Transitions Through Selective Depopulation of the Lower Laser Level by Means of Water Vapour", Phys. Lett. 18, 125 (1965).

19. Witteman, W. J. "High-Power Single Mode CO_2 Laser", IEEE J. Quantum Elec QE-4, 786 (1968).